LOCAL ENVIRONMENT DEPENDENCE OF MAGNETIC MOMENT IN Ni-Cu ALLOYS

A THESIS

Presented to

The Faculty of the Division of Graduate

Studies and Research

By

Rodrigo A. Medina

In Partial Fulfillment

of the Requirements for the Degree

Doctor of Philosophy

in the School of Physics

Georgia Institute of Technology

August 1976

LOCAL ENVIRONMENT DEPENDENCE OF MAGNETIC MOMENT

IN Ni-Cu ALLOYS

Approved:

Harold A. Gersch, Chairman

Joe W. Cable

Michael K. Wilkinson

Wallace C. Koehler

Date approved by Chairman: 20 Aug 1976

ACKNOWLEDGMENTS

The author would like to express his gratitude to the Instituto Venezolano de Investigaciones Científicas which supported him during his graduate studies. He is grateful for having at his disposal, during his thesis research, the excellent facilities of the Oak Ridge National Laboratory operated by the Union Carbide Corporation for the Energy Research and Development Administration. The author wishes to thank especially H. A. Gersch for the help and encouragement during the whole span of his graduate studies and J. W. Cable for the advice and many hours of fruitful discussions. He expresses his appreciation to M. K. Wilkinson for making possible his stay at ORNL and for serving on the thesis defense committee. He extends his sincere appreciation to W. C. Koehler and S. Spooner who were also members of the committee, to B. Mozer for making available the alloys used in this study, and to J. F. Cooke and J. S. Faulkner for providing the Ni and Ni-Cu densities of states. He also thanks R. M. Moon, E. O. Wollan, H. R. Child, T. Kaplan, M. Mostoller, J. W. Garland and A. Gonis for very useful discussions, J. L. Sellers for assistance in the experiment, and R. Burrell for the preparation of this manuscript.

a Paola

TABLE OF CONTENTS

TABLE OF CONTENTS (continued)

LIST OF TABLES

LIST OF FIGURES

LIST OF FIGURES (continued)

SUMMARY

The magnetic moments of nickel atoms in ferromagnetic Ni-Cu alloys are strongly dependent on their local environment. In this thesis is presented a study of this dependence determined by the magnetic diffuse scattering of polarized neutrons.

The unpolarized-neutron diffuse-scattering data have been traditionally analyzed with the linear superposition model of Marshall. An extension of this model, which includes the case of polarized neutrons and nonlinearities in the presence of short range order, is developed and used in the analysis of the data.

The measurements were carried out at 4.2 K on Ni-Cu samples with compositions 19.8, 29.6, and 52.5 at. % Cu. The data show that the copper atoms are not polarized and that the negative polarization existing between sites is associated with the neighboring Ni atoms. A comparison with the previous unpolarized-neutron data is presented.

An analytical expression for the polarized neutron cross section is obtained for a model in which the Ni moments are a function of the moments of the neighboring atoms. The formula gives a good description of the experimental cross sections. This magnetic-environment model also reproduces the moment disturbances of other dilute Ni based alloys. A Stoner type calculation shows that between 20 and 40% interatomic exchange is needed to reproduce the Ni-Cu magnetization and cross sections; within the same calculation each Cu atom induces a 1 - 2% moment reduction on its Ni neighbors for any given exchange field.

CHAPTER I

INTRODUCTION

The Ni based alloys have attracted attention for many years. Already in the 30's it was discovered that the binary alloys of many metals in Ni show a decrease of the average moment proportional to the impurity content.[1] These experiments were considered one of the most striking confirmations of the collective electron and rigid band models.[2-6] In particular, it was predicted that the extra electron provided by each copper atom added to nickel would fill a hole in the 3d band, thus reducing the moment by $g/2\ \mu_B$. For the same reasons it was also predicted that the addition of zinc, aluminum, or tin to nickel would produce a moment reduction of 2, 3, or 4 $g/2\ \mu_B$ per impurity atom; while the addition of cobalt would increase the moment by $g/2\ \mu_B$ per Co atom. All these predictions were in agreement with the observed moment variation.

The weakness of this theory became evident, however, when the neutron diffraction and diffuse scattering data of Shull and Wilkinson[7] showed the constancy of the individual moments in the Ni-Fe system. Similar results were found later in Ni-Co[8,9] and Co-Fe.[10,11] In this last case the moment of iron actually increases from 2.2 μ_B to 3.2 μ_B. The rigid-band theory proved to be unsatisfactory also in the Ni-Cu case because it neglects the repulsion between holes and copper atoms. Lang and Ehrenreich[12] proposed instead that this repulsion is actually dominant and prevents copper electrons from filling the holes on Ni atoms. This "minimum polarity" model was found to be in better agreement with

the magnetization and Curie temperature data than the rigid band model,[13] and it was later confirmed by the photoemission data[14,15] and CPA calculations[16,17] which explicitly show that the 3d densities of states of Ni and Cu keep their relative positions with respect to the Fermi energy in the whole range of concentrations. The main feature of these calculated and measured densities of states near the Fermi energy, the region that determines the magnetic behavior, is a peak due to the 3d nickel states of t_{2g} symmetry. On the other hand, the 3d states of Cu are well below the Fermi energy, are therefore occupied and have little effect on the Ni peak. The fact that the Cu levels are occupied implies also that the Cu is not polarized.

Another characteristic feature of Ni based alloys is the substantial dependence of the moments on their local environment, the most evident manifestation of which is the appearance of superparamagnetic clusters near the critical concentration for ferromagnetism. These effects can be probed directly with the magnetic diffuse scattering of neutrons. For example, the correlation between moments at different distances is measured with unpolarized neutrons, while the disturbances produced by an impurity on the surrounding moments is measured with polarized neutrons. Marshall[18] has shown that there is a simple relation between the moment-moment correlation and the moment disturbances if linear superposition of disturbances is assumed. Different measurements have been performed using the unpolarized neutron technique, e.g., Comly et al.[19] measured the moment disturbances produced in Ni by many different dilute impurities, with the exclusion of Cu. This last case was measured by Cable et al.[20] (20 at.% Cu) and by Aldred et al.[21]

(2-40 at.% Cu) in the ferromagnetic region while Hicks et al.[22] measured the scattering from the polarization clouds in the critical region.

All these measurements demonstrated that most nonmagnetic impurities produce a moment reduction extended to many neighbors. In the case of Cu, the element that produces the smallest moment reduction, the range of the disturbance increases steadily with increasing Cu content, and for 20 at.% Cu the disturbance already extends to fourth neighbors. Cable et al.[20] and Aldred et al.[21] analyzed their data with the linear superposition model of Marshall and obtained the average Ni and Cu moments. Their results deserve a more detailed discussion. The average moment within a copper cell was found to have the constant value of $-0.1\ \mu_B$ over the range 0-40 at.% Cu. This is a very surprising result because any simple theory will predict a rough scaling with the bulk average moment, which decreases by a factor of four in the same range (from 0.616 to $0.166\ \mu_B$). On the other hand, the moment density of pure nickel[23] is composed of a localized atomic-like magnetization superimposed on a uniform polarization of $-0.1\ \mu_B$/atom. Because of this and because of the evidence showing that the copper 3d shell is full, the negative moment obtained in the copper cells was identified with a uniform conduction band polarization. This interpretation is, however, inconsistent with the more recent Ni-Cu Bragg scattering data of Ito and Akimitsu,[24] which show that the uniform polarization is roughly proportional to the bulk moment. The discrepancy between the diffraction and diffuse scattering data was attributed by Ref. 24 to the linear superposition assumption of the Marshall model. Aldred et al.[21] themselves found that this assumption does not hold for the 50% alloy, while Garland and Gonis[25] have estimated

substantial nonlinearities for the correlations at concentrations bigger than 20 at.% Cu. A different analysis of the data and/or different experiments therefore seemed necessary. Since the diffuse scattering of polarized neutrons gives the moment disturbances directly and, in particular, yields the difference of average moments, $\langle\mu_{Cu}\rangle - \langle\mu_{Ni}\rangle$, without any model assumption, we decided to carry out new measurements on the Ni-Cu system with the polarized neutron technique. In this thesis, we present the moment disturbances measured in three ferromagnetic Ni-Cu alloys (19.8, 29.6, and 52.5 at.% Cu). The results obtained show that the Cu moment is indeed essentially zero and that the negative polarization is not truly uniform, being instead associated with the Ni atoms.

We have also developed a model for the interpretation of the data. The model assumes that the nickel moment depends on the local magnetic environment. An elementary argument showing why the nickel moment, unlike that of iron, depends substantially on the moments of neighboring atoms goes as follows. The energy and the hopping of electrons on or off an atom depends on whether the electron has its spin parallel or antiparallel to the spin of the atom. This difference, due to the Coulomb repulsion and the exclusion principle, favors the perpetuation of the atomic spin. On the other hand, Ni has only 0.6 d-holes per atom, which means that approximately 40% of the time the Ni atoms are in the configuration $3d^{10}$. Both spin states of electrons of this spin zero configuration are equivalent unless the neighboring atoms are polarized. The dependence of the Ni moment on the local magnetic environment can explain the strong and long-range moment reductions produced by nonmagnetic impurities. The moment reduction produced by the impurity on its neighbors is propagated to

neighbors of those neighbors and so on. The model developed here gives a good description of the measured moment disturbances.

CHAPTER II

CROSS SECTIONS AND EXACT RELATIONS

The disorder diffuse scattering of polarized neutrons from a ferromagnetic substitutional binary alloy, such as Ni-Cu, is composed of three kinds of processes: the nuclear scattering, the magnetic scattering, and the spin dependent nuclear-magnetic interference scattering. For neutrons polarized parallel ($\varepsilon = 1$) or antiparallel ($\varepsilon = -1$) to the magnetization, the cross section per atom may be written as:

$$\left(\frac{d\sigma}{d\Omega}\right)_{\varepsilon} = \left(\frac{d\sigma}{d\Omega}\right)_{N} + \varepsilon\left(\frac{d\sigma}{d\Omega}\right)_{NM} + \left(\frac{d\sigma}{d\Omega}\right)_{M}. \tag{1}$$

By measuring the cross sections for both polarizations and taking their difference, the interference term can be extracted. We have:

$$\Delta\frac{d\sigma}{d\Omega} = 2\left(\frac{d\sigma}{d\Omega}\right)_{NM}, \tag{2}$$

and

$$\sum_{\varepsilon}\left(\frac{d\sigma}{d\Omega}\right)_{\varepsilon} = 2\left(\frac{d\sigma}{d\Omega}\right)_{N} + 2\left(\frac{d\sigma}{d\Omega}\right)_{M}. \tag{3}$$

The diffuse nuclear scattering is proportional to the Fourier transform of the Cowley short-range order (SRO) parameters. More precisely, if c is the impurity concentration, $p_{\underline{m}}$ is the number of impurities at site $\underline{m}$ ($p_{\underline{m}} = 0,1$), and $\langle\cdots\rangle$ is the configurational average, then the SRO parameters are defined as:

$$c(1-c)\ \alpha(\underline{m}) = \langle(p_{\underline{m}+\underline{r}}-c)(p_{\underline{r}}-c)\rangle. \tag{4}$$

The nuclear scattering cross section is then given by

$$\left(\frac{d\sigma}{d\Omega}\right)_N = c(1-c)(\Delta b)^2\ S(\underline{K}), \tag{5}$$

where Δb is the difference of impurity and host nuclear scattering lengths

$$\Delta b = b_i - b_h, \tag{6}$$

and $S(\underline{K})$ is the SRO scattering function,

$$S(\underline{K}) = \sum_{\underline{m}} e^{i\underline{K}\cdot\underline{m}}\ \alpha(\underline{m}). \tag{7}$$

If the magnetization is perpendicular to the scattering plane, the magnetic cross section (in barns) is given by

$$\left(\frac{d\sigma}{d\Omega}\right)_M = c(1-c)\ T(\underline{K})(0.270)^2. \tag{8}$$

Here, $T(\underline{K})$ is a moment-moment correlation expressed in terms of $\mu_{\underline{n}}$ and $f_{\underline{n}}(\underline{K})$, the magnetic moment of the atom at site $\underline{n}$ and its form factor, respectively:

$$\mu_n(\underline{K}) = \mu_{\underline{n}}\ f_{\underline{n}}(\underline{K}) \tag{9}$$

$$c(1-c)\ T(\underline{K}) = \sum_{\underline{n}} e^{i\underline{K}\cdot\underline{n}} \langle \mu_{\underline{n}+\underline{r}}(\underline{K})(\mu_{\underline{r}}(\underline{K}) - \langle\mu(\underline{K})\rangle)\rangle. \tag{10}$$

Finally, the nuclear-magnetic interference term is proportional to a site-occupation magnetic-moment correlation. For a magnetization perpendicular to the scattering plane, we have

$$\left(\frac{d\sigma}{d\Omega}\right)_{NM} = 1/2\ \Delta\frac{d\sigma}{d\Omega} = c(1-c)\ \Delta b\ (0.540)\ M(\underline{K}) \tag{11}$$

and

$$c(1-c)\ M(\underline{K}) = \sum_{\underline{n}} e^{i\underline{K}\cdot\underline{n}} < (p_{\underline{n}+\underline{t}} - c)\ \mu_{\underline{t}}(\underline{K}) > \qquad (12)$$

where the quantity in brackets divided by c represents the average increase in the moment of the atom at site $\underline{t}$ when an impurity is located at site $\underline{n} + \underline{t}$.

The measurements performed on a polycrystalline sample give spherically averaged cross sections. The spherical average of $M(\underline{K})$, denoted (as any other spherical average) by dropping the vector symbol on K, complies with the following equation readily obtained from the definition (II.12).

$$M(K) = <\mu_i(K)> - <\mu_h(K)> + \text{DECAYING OSCILLATORY TERMS.} \qquad (13)$$

Here, $<\mu_i(K)>$ and $<\mu_h(K)>$ are the average impurity and host moments. We note that the large K values of M(K) give directly the difference of average moments. On the other hand, the spherically averaged unpolarized neutron cross section at large K gives the total moment fluctuation, which is composed of the difference of average moments plus the moment fluctuations of the two kinds of atoms.

$$\begin{aligned} T(K) = {} & \left(<\mu_i(K)> - <\mu_h(K)>\right)^2 \qquad (14) \\ & + <\left(\mu_i(K) - <\mu_i(K)>\right)^2>/(1-c) \\ & + <\left(\mu_h(K) - <\mu_h(K)>\right)^2>/c \\ & + \text{DECAYING OSCILLATORY TERMS.} \end{aligned}$$

There is also an exact relationship between the concentration derivative of the average moment and the scattering in the forward direction:

$$\frac{d\langle\mu\rangle}{dc} = M(0)/S(0). \tag{15}$$

The proof of this formula is presented in Appendix A, and is based on the following hypotheses: (1) It is assumed that the moments are determined by their local environment and (2) that the samples used to measure the concentration derivative have suffered the same heat treatment.

CHAPTER III

MANY-SITE PERTURBATIONS EXPANSION

Magnetic diffuse scattering is usually analyzed with the linear superposition model developed by Marshall[18] or with the Balcar and Marshall[26] model which includes some nonlinearities. We present here an extension of the above models, the many-site perturbations expansion, in which the moment on an atom is expanded as the average moment plus the linear superposition of perturbations produced by the kind of occupation of single sites, plus the extra perturbation produced by pairs of sites, plus the n-site perturbations. This procedure is particularly useful if the perturbations are small, so that the many-site perturbations are increasingly negligible. One of the advantages of this description is that it allows for a simple treatment of the effects of short-range order. We may write, for the random alloy,

$$\mu_{\underline{m}}(\underline{K}) = \bar{\mu}(\underline{K}) + \sum_{\underline{r}} \psi_1(\underline{K};\underline{r})(p_{\underline{m}+\underline{r}}-c) + 1/2! \sum_{\underline{r},\underline{t}} \psi_2(\underline{K};\underline{r},\underline{t})(p_{\underline{m}+\underline{r}}-c)(p_{\underline{m}+\underline{t}}-c) + 1/3! \sum_{\underline{r},\underline{t},\underline{n}} \psi_3(\underline{K};\underline{r},\underline{t},\underline{n})(p_{\underline{m}+\underline{r}}-c)(p_{\underline{m}+\underline{t}}-c)(p_{\underline{m}+\underline{n}}-c) + \cdots . \quad (1)$$

The moment disturbances $\psi_\alpha(\underline{K};\underline{r}_1,\underline{r}_2,\cdots,\underline{r}_\alpha)$ are symmetric functions of the arguments $\underline{r}_\lambda$ and they vanish if any two of the arguments are equal. The relationship between these parameters and the ones used by Balcar

and Marshall is given in Appendix B. With the use of the statistical independence of different sites and the following relationship:

$$(p_{\underline{n}}-c)^2 = (1-2c)(p_{\underline{n}}-c) + c(1-c) \tag{2}$$

we can easily prove that

$$\psi_\alpha(\underline{K};\underline{r}_1,\cdots,\underline{r}_\alpha) = [c(1-c)]^{-\alpha} \prod_{\lambda,\nu=1}^{\alpha} [1-(1-\delta_{\lambda\nu})\delta_{\underline{r}_\lambda \underline{r}_\nu}]$$

$$x \langle (p_{\underline{r}_1}-c)\cdots(p_{\underline{r}_\alpha}-c)\mu_{\underline{o}}(\underline{K})\rangle, \tag{3}$$

and that

$$\langle \mu(\underline{K})\rangle = \bar{\mu}(\underline{K}). \tag{4}$$

The diffuse scattering cross sections can be expressed in terms of the Fourier transforms of ψ_α, defined as follows:

$$\Psi_\alpha(\underline{K};\underline{r}_1,\cdots,\underline{r}_{\alpha-1}) = \sum_{\underline{m}} e^{i\underline{K}\cdot\underline{m}} \psi_\alpha(\underline{K};\underline{r}+\underline{m},\cdots,\underline{r}_{\alpha-1}+\underline{m},\underline{m}). \tag{5}$$

In fact, from equation (III.3) and the definition of $M(\underline{K})$ in (II.12), one gets

$$M(\underline{K}) = \Psi_1(\underline{K}), \tag{6}$$

while, by multiplying expansion (III.1) by $\mu_{\underline{o}}$, taking the average, and using (III.3), one obtains

$$\langle \mu_{\underline{m}}(\underline{K})\mu_{\underline{o}}(\underline{K})\rangle = \bar{\mu}(\underline{K})^2 + c(1-c) \sum_{\underline{r}} \psi_1(\underline{K};\underline{r})\ \psi_1(\underline{K};\underline{r}+\underline{m})$$

$$+ \frac{c^2(1-c)^2}{2!} \sum_{\underline{r},\underline{t}} \psi_2(\underline{K};\underline{r},\underline{t})\ \psi_2(\underline{K};\underline{r}+\underline{m},\underline{t}+\underline{m})$$

$$+ \frac{c^3(1-c)^3}{3!} \sum_{\underline{r},\underline{t},\underline{n}} \psi_3(\underline{K};\underline{r},\underline{t},\underline{n})\ \psi_3(\underline{K};\underline{r}+\underline{m},\underline{t}+\underline{m},\underline{n}+\underline{m}) + \cdots \tag{7}$$

This gives the unpolarized neutron cross section by a Fourier transformation (see definitions (II.10) and (III.5)):

$$T(\underline{K}) = |\Psi_1(\underline{K})|^2 + \frac{c(1-c)}{2!} \sum_{\underline{r}} |\Psi_2(\underline{K};\underline{r})|^2 + \frac{c^2(1-c)^2}{3!} \sum_{\underline{r},\underline{t}} |\Psi_3(\underline{K};\underline{r},\underline{t})|^2 + \cdots \quad . \tag{8}$$

Note that, for the random alloy, the interference term in the cross section, $M(\underline{K})$, contains only the single-site perturbations. Note also that, if the many-site perturbations are negligible, $T(K)$ is just the square of $M(K)$. This relationship breaks down when the many-site perturbations are important; for example, we should expect this to happen near the critical composition of Ni-Cu.

For the random alloys, one can generalize the equation (II.15) to higher derivatives of the average moment:

$$\frac{d^n\langle\mu\rangle}{dc^n} = \sum_{\underline{r}_1,\cdots,\underline{r}_n} \psi_n(0;\underline{r}_1,\cdots,\underline{r}_n) = \sum_{\underline{r}_1,\cdots,\underline{r}_{n-1}} \Psi_n(0;\underline{r}_1,\cdots,\underline{r}_{n-1}). \tag{9}$$

The proof of this equation for n = 2 is given in Appendix C.

When short-range order is present, we can still use the expansion (III.1) if we treat the introduction of SRO as a perturbation on the random alloy; this treatment may, of course, become inaccurate near the critical composition of Ni-Cu. The expansion is therefore done in terms of the parameters the alloy would have if it were random and the SRO introduced only into the process of averaging.

The average moment in the presence of SRO is obtained by taking the average of (III.1)

$$\langle \mu(\underline{K}) \rangle = \bar{\mu}(\underline{K}) + \frac{c(1-c)}{2!} \sum_{\underline{r},\underline{t}} \psi_2(\underline{K};\underline{r},\underline{t}) \alpha(\underline{r}-\underline{t}) + \frac{c(1-c)}{3!} \sum_{\underline{r},\underline{t},\underline{n}} \psi_3(\underline{K};\underline{r},\underline{t},\underline{n}) \eta(\underline{r}-\underline{n},\underline{t}-\underline{n}) + \cdots \qquad (10)$$

Here, we have introduced the 3-site SRO parameters $\eta(\underline{r},\underline{t})$ which are defined by

$$c(1-c)\, \eta(\underline{r},\underline{t}) = (1-\delta_{\underline{r}\underline{o}})(1-\delta_{\underline{t}\underline{o}})(1-\delta_{\underline{r}\,\underline{t}}) \langle (p_{\underline{r}}-c)(p_{\underline{t}}-c)(p_{\underline{o}}-c) \rangle . \qquad (11)$$

These parameters satisfy the following symmetry relationships:

$$\eta(\underline{r},\underline{t}) = \eta(\underline{t},\underline{r}) = \eta(\underline{r}-\underline{t},-\underline{t}), \qquad (12)$$

and they are related to the concentration derivative of the 2-site SRO parameters, $\alpha(\underline{n})$, by the sum rule

$$\sum_{\underline{m}} \eta(\underline{n},\underline{m}) = (1-\delta_{\underline{n}\,\underline{o}})\{(1-2c)[S(0)-2] + (1-c)cS(0)\frac{d}{dc}\}\, \alpha(\underline{n}) . \qquad (13)$$

This can be proved by using the method of Appendix A. The presence of SRO also modifies the polarized neutron cross section. From (III.1), one obtains

$$\begin{aligned} \langle (p_{\underline{n}}-c)\mu_{\underline{o}}(\underline{K}) \rangle &= \sum_{\underline{r}} \psi_1(\underline{K};\underline{r}) \langle (p_{\underline{n}}-c)(p_{\underline{r}}-c) \rangle \\ &\quad + \frac{1}{2!} \sum_{\underline{r},\underline{t}} \psi_2(\underline{K};\underline{r},\underline{t}) \langle (p_{\underline{n}}-c)(p_{\underline{r}}-c)(p_{\underline{t}}-c) \rangle + \cdots \\ &= c(1-c) \sum_{\underline{r}} \psi_1(\underline{K};\underline{n}) \alpha(\underline{r}-\underline{n}) \\ &\quad + c(1-c)(1-2c) \sum_{\underline{r}} \psi_2(\underline{K};\underline{r},\underline{n}) \alpha(\underline{r}-\underline{n}) \\ &\quad + \frac{c(1-c)}{2} \sum_{\underline{r},\underline{t}} \psi_2(\underline{K};\underline{r},\underline{t}) \eta(\underline{r}-\underline{n},\underline{t}-\underline{n}) + \cdots . \end{aligned} \qquad (14)$$

for which the Fourier transform is $M(\underline{K})$, i.e.,

$$M(\underline{K}) = S(\underline{K})\ \Psi_1(\underline{K}) + (1-2c)\ V(\underline{K}) + U(\underline{K}) + \cdots \tag{15}$$

$$V(\underline{K}) = \sum_{\underline{r},\underline{n}} e^{i\underline{K}\cdot\underline{n}}\ \psi_2(\underline{K};\underline{r},\underline{n})\ \alpha(\underline{r}-\underline{n}) \tag{16}$$

$$U(\underline{K}) = \frac{1}{2} \sum_{\underline{r},\underline{t}} \psi_2(\underline{K};\underline{r},\underline{t}) \sum_{\underline{n}} e^{i\underline{K}\cdot\underline{n}}\ \eta(\underline{r}-\underline{n},\underline{t}-\underline{n}) \tag{17}$$

In Appendix D, we show that, in the case of clustering induced in a system in thermal equilibrium by pairwise forces, $U(\underline{K})$ can be approximated by

$$U(\underline{K}) \simeq (1-2c)(S(\underline{K})-1)\ V(\underline{K}) \tag{18}$$

in which case $M(\underline{K})$ assumes the form

$$M(\underline{K}) = S(\underline{K})[\Psi_1(\underline{K}) + (1-2c)\ V(\underline{K})] + \cdots \tag{19}$$

With similar, but more complicated algebra shown in Appendix E, one finds

$$T(\underline{K}) = S(\underline{K})[\Psi_1(\underline{K}) + (1-2c)\ V(\underline{K})]^2 + \text{Terms in } (\psi_2)^2. \tag{20}$$

This is equivalent to the formula given by Marshall[18] that was used to analyze the previous Ni-Cu data.[20,21] Again, if 2-site disturbances are small, polarized and unpolarized neutrons give the same information.

In the case of polycrystalline samples, the measurements give spherical averages. The analysis of this case is simplified when the difference among the form factors is neglected. In the Ni-Cu case, where $\mu_{Cu} = 0$, this approximation neglects only the environmental dependence of the form factor. We may write:

$$\bar{\mu}(\underline{K}) = \langle f(\underline{K}) \rangle\ \bar{\mu} \tag{21}$$

$$\psi_\alpha(\underline{K};\underline{r}_1,\cdots,\underline{r}_\alpha) = \langle f(\underline{K})\rangle\ \phi_\alpha(\underline{r}_1,\cdots,\underline{r}_\alpha). \tag{22}$$

Equation (III.19) then becomes:

$$M(\underline{K}) = \langle f(\underline{K})\rangle\ S(\underline{K}) \sum_{\underline{m}} \gamma(\underline{m})\ e^{i\underline{K}\cdot\underline{m}} \tag{23}$$

where

$$\gamma(\underline{m}) = \phi_1(\underline{m}) + (1-2c) \sum_{\underline{m}} \phi_2(\underline{r},\underline{m})\ \alpha(\underline{r}-\underline{m}). \tag{24}$$

If we neglect the asphericity of $f(\underline{K})$, the spherical average is given by:

$$M(K) \simeq \langle f(K)\rangle \sum_{\underline{m}} \gamma(\underline{m}) \sum_{\underline{r}} \alpha(\underline{r})\ j_o(K|\underline{r}+\underline{m}|). \tag{25}$$

We use this equation to obtain the random moment perturbation $\phi_1(K)$ for comparison with the magnetic environment model of Chapter VI.

A simplified version of (III.24) is obtained when the two-site perturbations are small and the impurity moment is zero. In that case

$$\phi_2(\underline{r},\underline{m}) \simeq -\left(\phi_1(\underline{r})\ \delta_{\underline{m}o} + \phi_1(\underline{m})\ \delta_{\underline{r}o}\right)(1-\delta_{\underline{r}\,\underline{m}})/(1-c) \tag{26}$$

and

$$\gamma(0) = \phi_1(0) - \frac{1-2c}{1-c} \sum_{\underline{r}\neq 0} \phi_1(\underline{r})\ \alpha(\underline{r})$$

$$\gamma(\underline{m}) = \phi_1(\underline{m})\ \left[1 - \frac{1-2c}{1-c}\ \alpha(\underline{m})\right], \text{ for } \underline{m} \neq 0. \tag{27}$$

CHAPTER IV

EXPERIMENTAL PROCEDURES AND CORRECTIONS

The Samples

Three ferromagnetic samples of ^{62}Ni-Cu alloys with 19.8 at.%, 29.6 at.%, and 52.5 at.% Cu were used in these experiments. Two different chemical analyses of the last sample gave results of 53.5 and 52.5 at.% Cu. Our magnetization measurement on this sample ($0.0490 \pm 0.0025\ \mu_B$) is consistent with the second result. The isotope ^{62}Ni was chosen because its negative scattering length gives a large Δb. The isotopic composition of the enriched nickel was, in atomic %: ^{62}Ni, 99.06%; ^{58}Ni, 0.34%; ^{60}Ni, 0.034%; ^{61}Ni, 0.12%; ^{59}Ni, <0.05%. The main magnetic impurities present were Fe >0.001% but <0.01% and Mn <0.01%. Other impurities were Zn <0.2% and Th <0.2%. The nickel was combined with natural 99.995% copper. The incoherent scattering cross section of the nickel, and the copper-nickel scattering length difference, calculated by taking into account the isotopic composition, are $\sigma\ \text{inc}/4\pi = 0.0275 \pm 0.0002$ barn and $\Delta b = 1.621 \pm 0.02$ 10^{-12} cm.

The samples were polycrystalline plates about 1.5 mm thick. They were prepared by arc-melting in a berylia crucible under an argon atmosphere, rolling the button to 70% of its thickness, annealing at 1050°C for 16 hrs and quenching. All neutron measurements were performed at 4.2 K. By the interpolation of published data,[27] we estimated the following 4.2 K lattice parameters: for the 20% sample, a = 3.532 Å; 30%, a = 3.54 Å, and 52.5%, a = 3.56 Å.

Equipment and Experimental Conditions

The experiments were carried out on the polarized neutron diffractometer at HB-1 of the High Flux Isotope Reactor at the Oak Ridge National Laboratory. A schematic drawing of the diffractometer is shown in Fig. 1. A monochromatic beam having wave length 1.067 Å and 99% vertical polarization is obtained by reflection from a magnetized Co-Fe (200) monochromator. The incident beam illuminates the sample mounted in symmetrical transmission geometry inside a cryostat. The sample temperature was kept at 4.2 K. Two superconducting coils permit the application of a vertical magnetic field to the sample. For the 20% and 30% samples a field of 25 kOe was used, while measurements at 10 kOe and 57 kOe were taken for the 52.5% alloy. The polarization of the beam can be inverted by applying a radiofrequency horizontal field within a coil traversed by the incident beam before the cryostat. The diffuse scattering is measured with a two-axis arrangement, (i.e. no analyzing crystal, $2\theta_A = 0$, and scanning of the angle ϕ); a Be (110) analyzer in the zero energy transfer condition was, however, used in order to prevent the incident beam from crossing the counter shielding at the smaller angles ($\phi \leq 2.5°$).

Procedures and Instrumental Corrections

The scattering of both neutron polarizations, parallel and antiparallel to the magnetic field, was measured inside the first Bragg peak. The measurements were taken each half degree within the range $1.5° \leq \phi \leq 27.5°$. The spin-dependent transmission of the samples, needed for calculating the beam attenuation, was also measured.

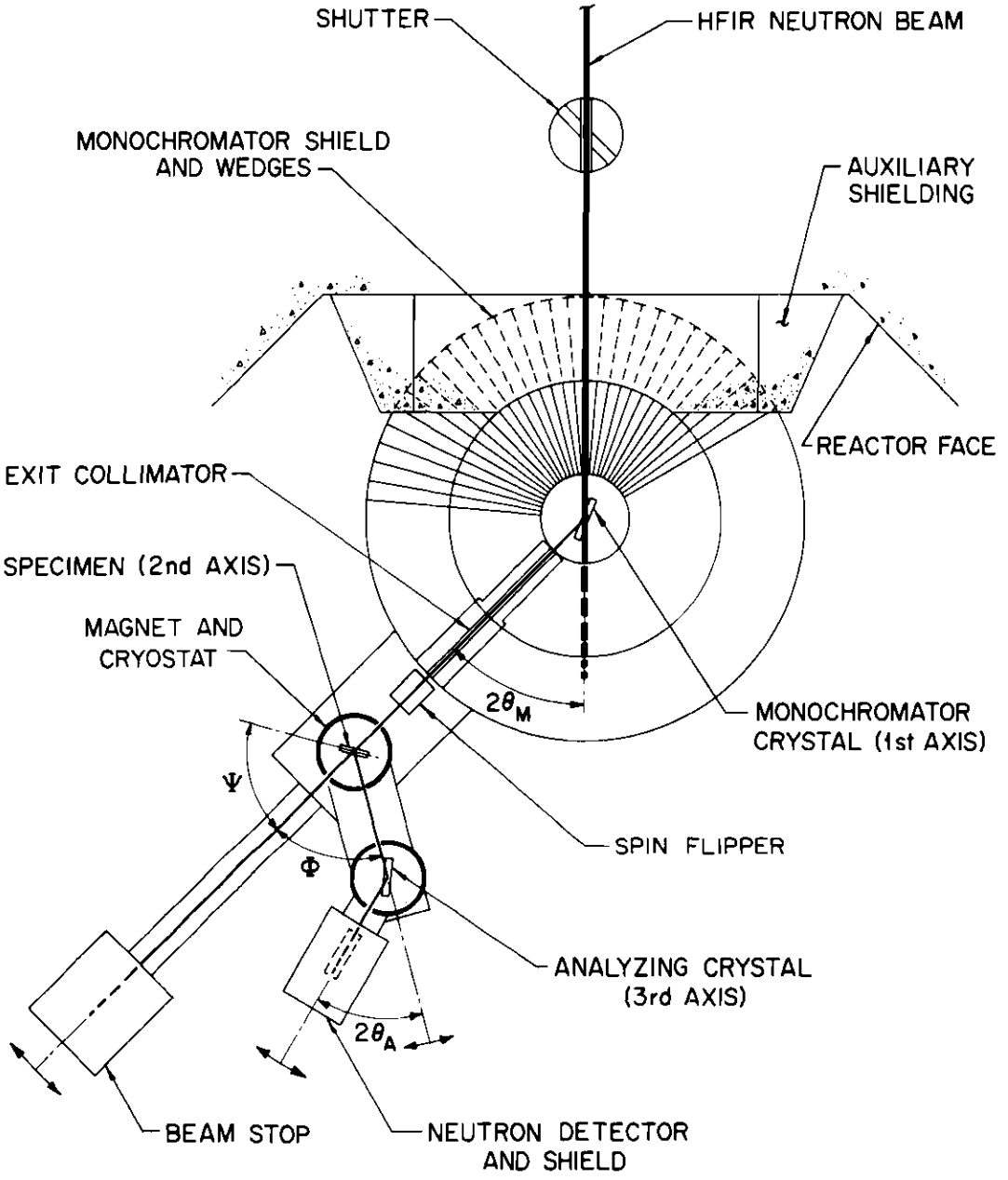

Figure 1. HB-1 Polarized Neutron Spectrometer

The measured intensites must be corrected by subtraction of the instrumental background. This background is mainly due to the air scattering of the transmitted beam, which is attenuated by the sample, but it also contains neutrons from other sources, such as fast neutrons, scattering from the cryostat, etc., which are sample independent. Two measurements are, therefore, needed to separate the two components of the background, one with a cadmium plate replacing the sample and the other with no sample at all. The intensities were calibrated by measuring the scattering of a vanadium plate, a material that has a large incoherent scattering cross section. The triple-axis small-angle data were calibrated by comparison with two-axis data in an overlap region (2.5-3.5°). The sum and the difference of the cross sections of the two spin states were then calculated taking into account attenuation and the polarization of the beam. No beam depolarization due to the samples was observed.

Other Contributions to the Scattering

The following processes contribute to the scattering: (1) disorder diffuse scattering, nuclear and magnetic as explained in Chapter II, (2) incoherent scattering, (3) multiple scattering, (4) thermal diffuse scattering. This last contribution is negligible at the temperatures and wave vectors of these experiments. The incoherent scattering is spin independent and therefore, it contributes only to the sum cross section. This contribution was calculated and then subtracted. More troublesome is the multiple scattering contribution. The standard method[28] assumes isotropic scattering, in which case the multiple scattering is a function of two quantities only, the logarithm of the transmission, $\tau = \ln T$, and

the ratio, ω, of the scattering cross section to the total cross section. The total cross section is proportional to τ while the scattering cross section is the total minus the absorbtion cross sections; ω is therefore a function of τ and the absorbtion cross section. Reference 28 gives a tabulation of the multiple scattering for different values of τ and ω that were used to calculate the multiple scattering. The fact that the transmission depends on the neutron polarization implies that there is a multiple scattering contribution to the difference cross section. The validity of this procedure for calculating the multiple scattering, i.e. the validity of using the isotropic scattering approximation, can be checked by comparison of the K-independent term of the measured nuclear diffuse scattering with its theoretical value. The measured value is obtained in the analysis of the data as explained in Chapter V. These values are shown in Table 1 together with the other contributions to the sum and difference cross sections. The agreement is good for the 19.8 and 29.6% data but not for the 52.5% data which were overcorrected. However, in this last case the multiple scattering contribution to the difference cross sections is negligible, and therefore the discrepancy has no consequences.

Resolution

The expression given in Chapter II for the difference cross section assumes that the magnetization is perpendicular to the scattering vector, i.e., it is valid only for perfect vertical resolution. In a more general case, the measured cross section is:

$$\left(\Delta\frac{d\sigma}{d\Omega}(K)\right)_{\text{measured}} = \int_{-\infty}^{\infty} dW \, \frac{K^2}{K^2+W^2} \, \frac{e^{-(W/\eta)^2}}{\sqrt{\pi}\,\eta} \, \Delta\frac{d\sigma}{d\Omega}\left(\sqrt{K^2+W^2}\right) \qquad (1)$$

Table 1. Contributions to the Sum and Difference Cross Sections (in mb)

c	ΔMS[a]	ΣMS[b]	Incoherent	$2c(1-c)\ (\Delta b)^2$ calc.	meas.[c]
0.198	15.3 (4.4)	171 (46)	63 ± 6	833 (21)	838 (3)
0.296	9 (11)	201 (42)	67 ± 9	1095 (27)	1040 (9)
0.525	0 (13)	245 (47)	76 ± 17	1310 (33)	1166 (3)

a. Multiple scattering contribution to $\Delta d\sigma/d\Omega$.

b. Multiple scattering contribution to $\Sigma d\sigma/d\Omega$.

c. Error shown is the statistical uncertainty.

where K is the component of the scattering vector perpendicular to the magnetization, W is the parallel component, and a gaussian vertical resolution of width $2\sqrt{\ln 2}\,\eta$ is assumed. A direct measurement of η and a geometrical calculation lead to essentially the same value, $\eta = 0.12\ \text{Å}^{-1}$. The integral equation (IV.1) can be analytically inverted:

$$\Delta\frac{d\sigma}{d\Omega}(K) = \frac{\eta}{\sqrt{\pi}} K^2 e^{(K/\eta)^2} \int_K^\infty \frac{dW}{W} e^{-(W/\eta)^2} (W^2-K^2)^{-\frac{1}{2}} \left[\frac{2}{W^2}+\frac{2}{\eta^2} - \frac{1}{W}\frac{d}{dW}\right] \left(\Delta\frac{d\sigma}{d\Omega}(W)\right)_{meas.} \tag{2}$$

The difference cross section was corrected with the method of spline functions.[29] The raw data were fitted with a smooth curve that was then used to calculate the correction with equation (IV.2). Figures 2 and 3 show an example of raw and corrected data. The difference is as large as 15% for the innermost points.

The sum cross section is also slightly affected by the vertical resolution. This effect can be approximately corrected by shifting the transferred momentum according to the formula

$$K_{cor} = \sqrt{K^2 + \eta^2/2}. \tag{3}$$

The horizontal resolution has a negligible effect in both cases.

Magnetic Contribution to the Sum Cross Section

The sum cross section, as previously explained, is composed of a nuclear and a magnetic term. The large value of Δb of the samples insures that the magnetic contribution is only a small fraction of the sum cross section. It is therefore a proper approximation to use equations (III.19) and (III.20) to calculate the magnetic term from the difference cross section. We obtain from (II.3), (II.5), and (II.8)

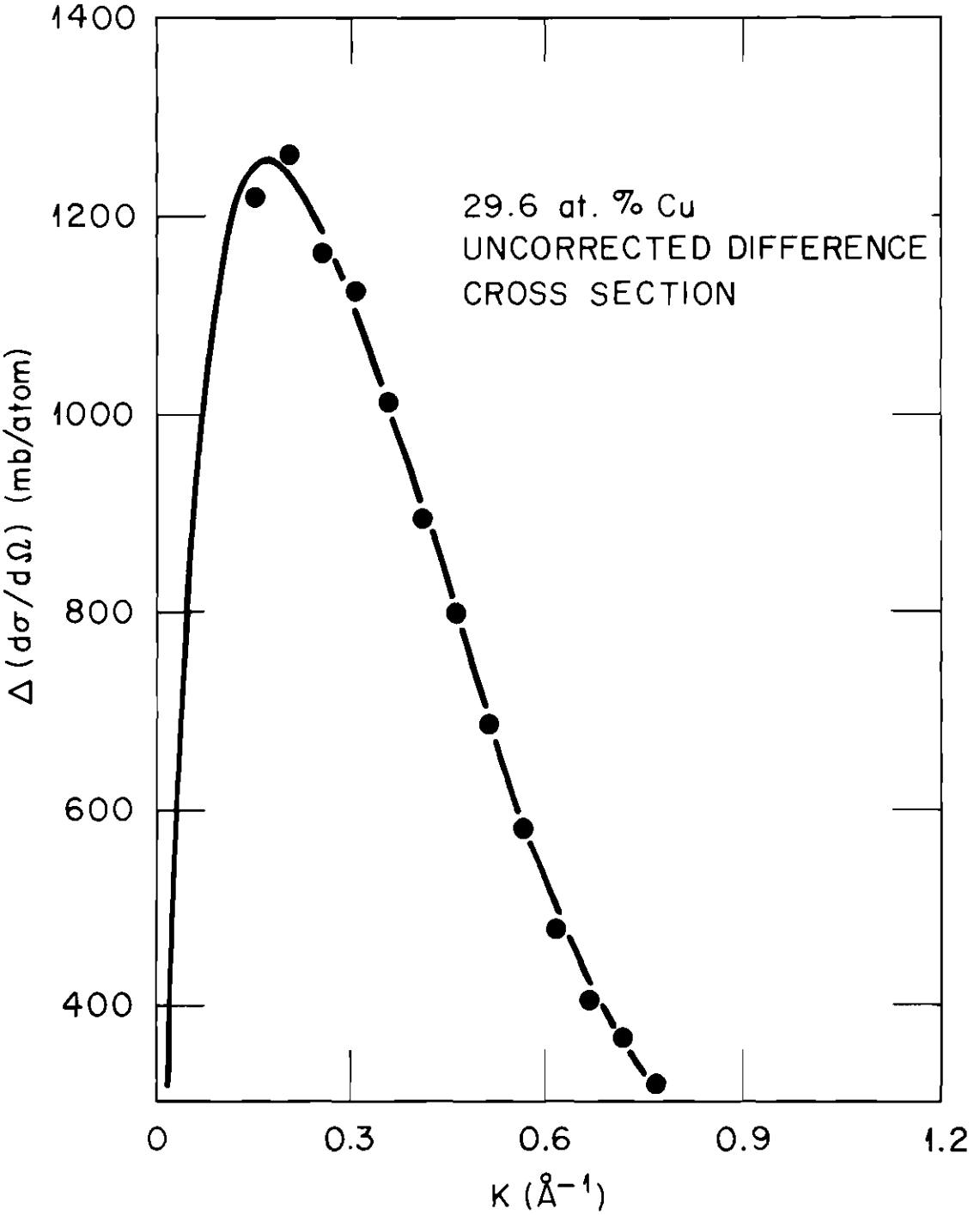

Figure 2. Example of Uncorrected Difference Cross Section

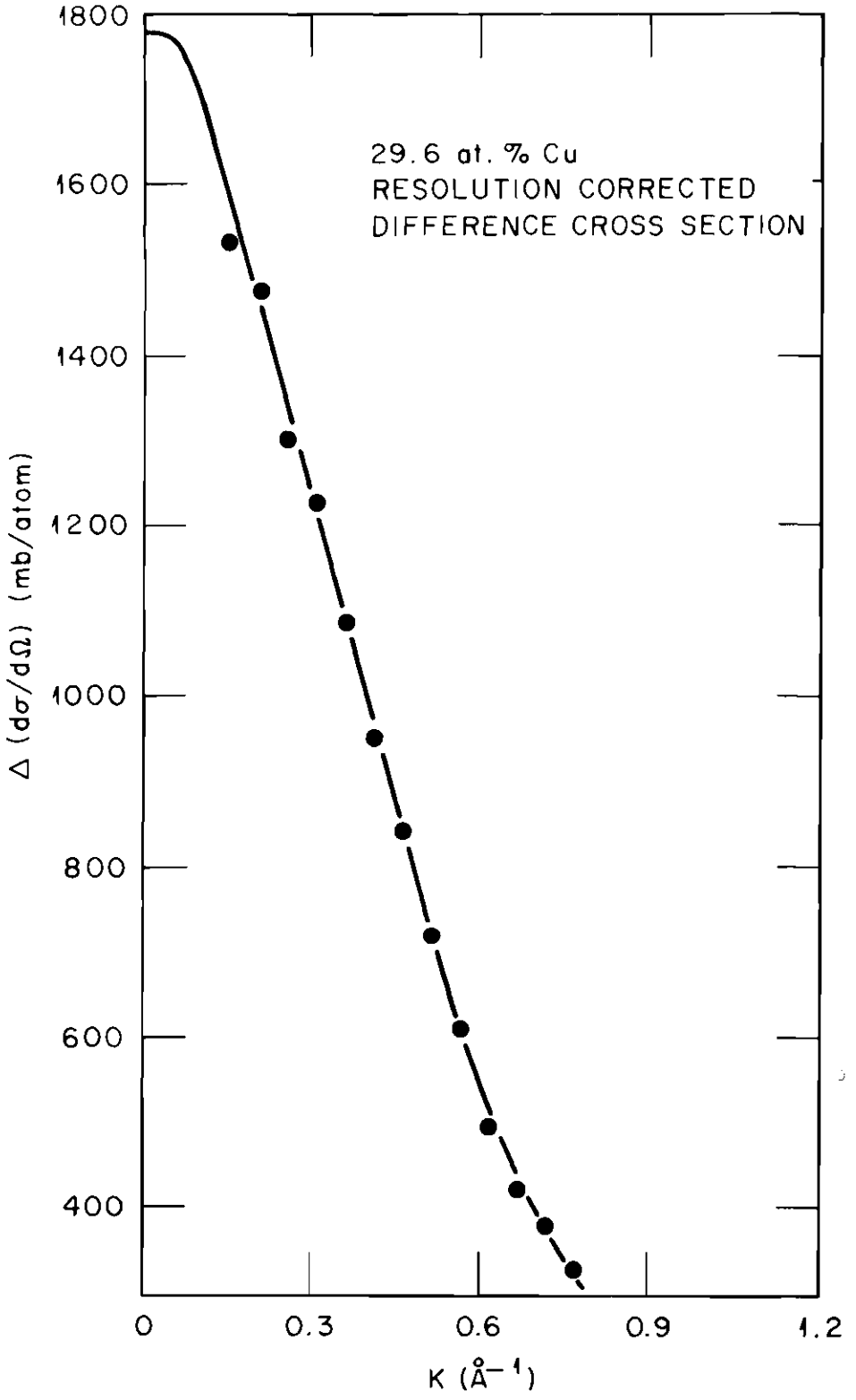

Figure 3. Example of Resolution Corrected Difference Cross Section

$$\sum_{\varepsilon} \left(\frac{d\sigma}{d\Omega}\right)_{\varepsilon} \simeq 2\left(\frac{d\sigma}{d\Omega}\right)_{N} + 1/8\ \left[\Delta\frac{d\sigma}{d\Omega}\right]^2 / \left(\frac{d\sigma}{d\Omega}\right)_{N}. \qquad (4)$$

This equation was used to calculate the nuclear cross section.

Magnetization Measurement

Near the critical region the magnetic properties of Ni-Cu alloys are strongly concentration and SRO dependent. We therefore measured the magnetization of the 52.5 at.% Cu alloy instead of using the published magnetization data. A needle-shaped specimen was prepared from the same material used in the diffraction experiment, and its magnetization was measured with the ballistic method at 4.2 K and different fields. The experiment was calibrated with a superconducting niobium needle of approximately the same shape. The magnetization as a function of field is shown in Fig. 4. The magnetization at the field of the neutron measurement (10 kOe) is 40.1 ± 2 G which corresponds to 0.049 ± 0.0025 μ_B per atom.

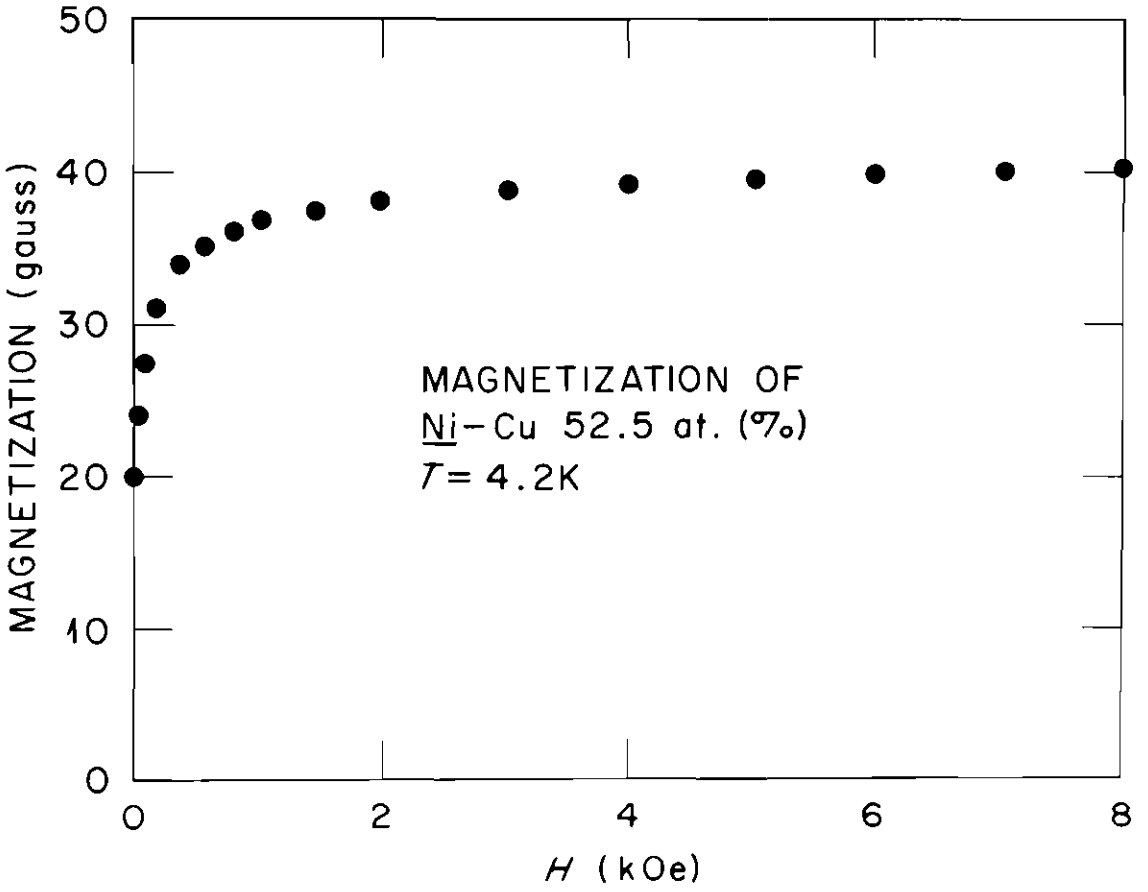

Figure 4. Magnetization of Ni-Cu 52.5 at. %

CHAPTER V

DIRECT EXPERIMENTAL RESULTS

Short-Range Order

The Ni-Cu alloys exhibit substantial clustering that must be taken into account when considering the magnetic moment distributions. We therefore must first obtain the SRO parameters from the data. This is accomplished by fitting the nuclear cross section with a function of the following form:

$$[c(1-c)(\Delta b)^2]^{-1} \left(\frac{d\sigma}{d\Omega}\right)_N = S(K) = \sum_{\lambda} \alpha(R_\lambda)\ Z_\lambda j_o(KR_\lambda). \qquad (1)$$

Here Z_λ is the coordination number and R_λ is the radius of the shell. Theoretically $\alpha(0) = 1$, but in the fitting we consider it as a free parameter to compensate for any possible error in the determination of the incoherent and multiple scattering that was subtracted to obtain the nuclear cross section. The results of the fittings are given in Table 2 and Fig. 5. For the 29.6% alloy, it was necessary to use up to nine shells in order to get a good fit with reasonably small SRO parameters; in this case the parameters were constrained to be small. Comparison of our results with those of Aldred et al.,[21] Cable et al.,[20] and Mozer et al.[30] shows that the SRO parameters of these samples are slightly larger than those previously reported. This is not surprising because the SRO may be sample dependent. There is also a difference in the sign of $\alpha(R_2)$ between our results and some of the previous results.[20,21]

Table 2. SRO Parameters

c	0.198	0.296	0.525
α_0	1.006 (4)	0.950 (9)	0.890 (3)
α_1	0.1175 (35)	0.1432 (82)	0.1335 (33)
α_2	-0.0614	-0.0328	-0.0747
α_3	0.0445	0.0432	0.0436
α_4	-0.0584	-0.0098	-0.0479
α_5	0.0263	0.0108	0.0148
α_6		0.0225	
α_7		0.0037	
α_8		-0.0211	
α_9		0.0065	
X^2/N	1.3	0.97	0.80

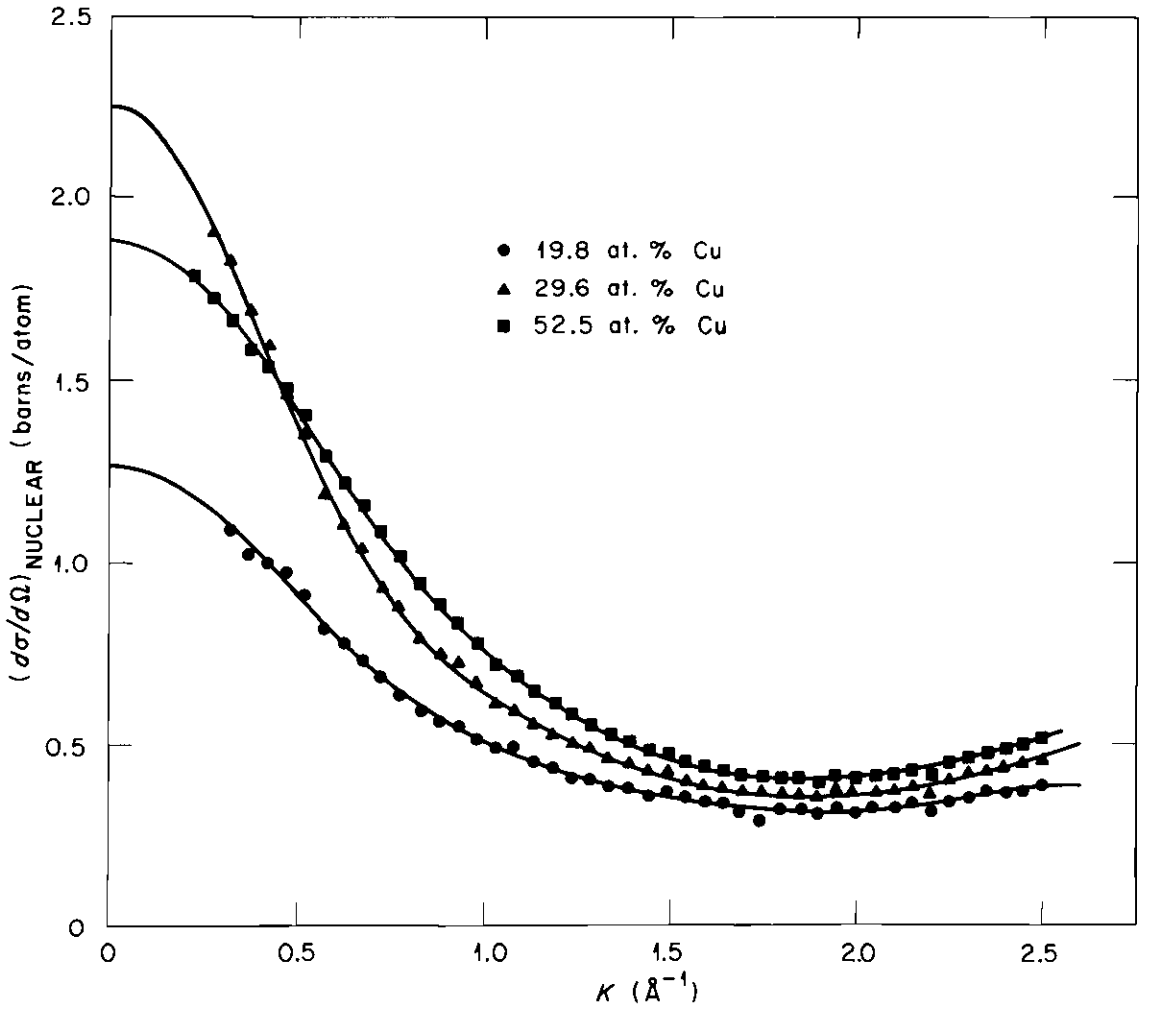

Figure 5. Nuclear Diffuse Scattering Cross Sections of Ni-Cu Alloys

It should be noted that, because of the larger nuclear cross sections of our samples and/or the larger range in K values of our data, the present SRO results should be more accurate than those obtained in references 20 and 21. Nevertheless, all of the SRO measurements indicate that clustering is present in these alloys.

The Negative Magnetization Is Not Uniform

The main result that can be obtained from the data is the solution of the apparent discrepancy between the diffraction data and the unpolarized neutron diffuse scattering data. The Bragg scattering results for pure Ni by Mook[23] and for Ni-Cu by Ito and Akimitsu[24] show that the average moment density is composed of a local atomic-like moment density and a uniform negative magnetization between sites. The Ito and Akimitsu data indicate that the uniform magnetization decreases monotonically with increasing Cu content and is roughly proportional to the local moment. On the other hand, the unpolarized neutron experiments[20,21] were interpreted to imply the existence of a uniform moment and/or a local Cu moment totaling $-0.1\ \mu_B$ over the range 0-40 at.% Cu. The moment values that we obtain from our polarized neutron data, which are more easily analyzed, are in agreement with the diffraction data.

In previous analyses of Ni-Cu diffuse scattering data,[20,21] it was assumed that the negative magnetization not seen in diffraction experiments is truly uniform and therefore unobservable even by diffuse scattering experiments. Consequently, a local atomic or ionic form factor was assigned to all observed moments. If this assumption were true, the quantity $M(0)/S(0)$ should be equal to the concentration derivative

of the local moment, now known to be approximately -1.35 μ_B. To the contrary, our polarized neutron scattering data clearly show that M(0)/S(0) is equal to the concentration derivative of the bulk moment (see Table 3). This confirms the theoretical argument made elsewhere[31] that the negative magnetization in alloys consists only of short-range contributions from each magnetic atom. Its form factor, although negligible at Bragg peaks, can be seen by diffuse neutron scattering. This result was suggested only ambiguously by the analysis of the earlier unpolarized neutron scattering data.[20,21]

Form Factor

According to the previous discussion, the Ni form factor is composed of a local form factor $f_\ell(\underline{K})$ observed in the Bragg peaks, and the "non-local" form factor $f_{n-\ell}(\underline{K})$ associated with the negative magnetization between atoms. If α is defined as the fraction of nonlocal moment, we have:

$$f(\underline{K}) = (1 + \alpha)\, f_\ell\, (\underline{K}) - \alpha f_{n-\ell}\, (\underline{K}). \qquad (2)$$

The negative magnetization was originally attributed to s-p band polarization ("conduction" moment). On the other hand, Moon[32] has shown that in the tight-binding band approximation the 3d form factor assumes the form of equation (V.2) where the local form factor is calculated with atomic 3d orbitals, and the nonlocal part is a linear combination of overlap integrals with 3d orbitals of neighboring atoms. These have the form

$$\int d^3r\, \phi^*_\lambda(\underline{r})\, \phi_\mu(\underline{r}-\underline{\rho})\, e^{i\underline{K}\cdot\underline{r}}.$$

Table 3. Direct Experimental Results

c	0.198	0.296	0.525	0.525
$H(k0_e)$	25	25	10	57
$\langle\mu_{Ni}\rangle-\langle\mu_{C\mu}\rangle$ [(a)]	0.478 (5)	0.413 (6)	0.091 (2)	0.106 (2)
$\langle\mu\rangle/(1-c)$	0.486 (3)	0.397 (6)	0.103 (5)	0.114 (6)
$M(0)/S(0)$	-1.125 (10)	-1.128 (10)	-0.65 (2)	-0.72 (2)
$d\langle\mu\rangle/dc$	-1.140 (10)	-1.120 (10)	-0.66 (2)	-0.79 (6)
$\langle\mu_{C\mu}\rangle$	0.006 (13)	-0.011 (12)	0.006 (7)	0.004 (7)

(a) A multiple scattering uncertainty of 0.015 μ_B must be added to the statistical error quoted.

As explained in detail elsewhere,[31] both conduction and overlap moment lead to very similar nonlocal form factors as shown in Fig. 6. However, the concentration dependence of α in Ni-Cu permits discrimination between the two possibilities. If the nonlocal moment were due to conduction-band polarization, it would be proportional to the local Ni moment, and therefore α should be roughly constant. On the other hand, if the nonlocal moment were due to d-d overlap, α should decrease with a decreasing number of Ni-Ni bonds. Assuming overlap to arise only between two Ni atoms, one finds

$$\langle\alpha\rangle = \alpha_o(1-c), \tag{3}$$

where $\alpha_o = 0.154$ is the pure nickel α. The average $\langle\alpha\rangle$ is the proper value for the analysis of the diffuse scattering, while a slightly different form α_{eff} must be used for the diffraction data.[31] We show in Fig. 7 that the Bragg scattering of References 23 and 24 favors Moon's d-d overlap assumption, which we therefore follow in the data analysis. We calculated the spherically averaged overlap form factor from published wave function calculations,[31] while for the local form factor we used the same as that used by Mook.[22] We neglect the difference between the Ni and Cu form factors in the analysis of the moment disturbances. This introduces no error because the Cu moment is negligible.

Moment Disturbances

The nuclear-magnetic interference cross section is analyzed in three different ways. First, in order to obtain the average moments, it is fitted with the following expression, obtained by taking the spherical average of (II.12):

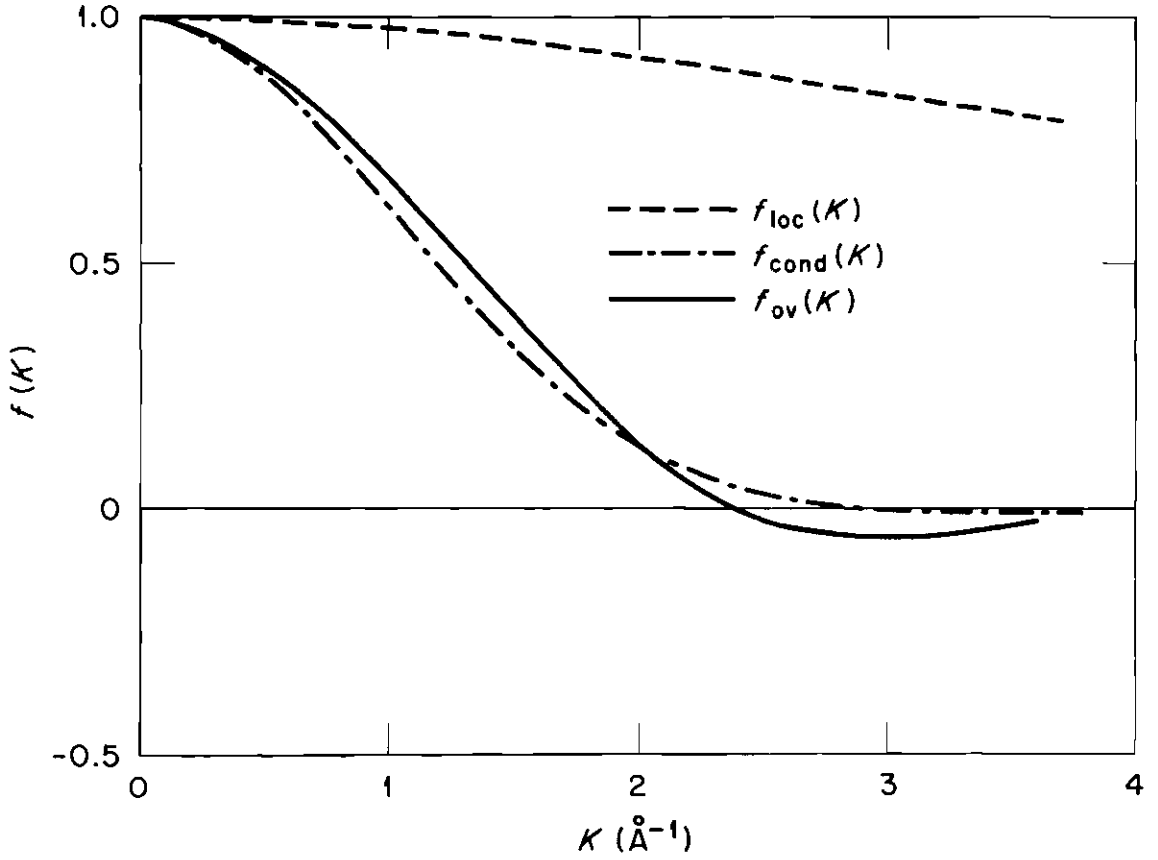

Figure 6. Spherically Averaged Local and Nonlocal Form Factors of Ni

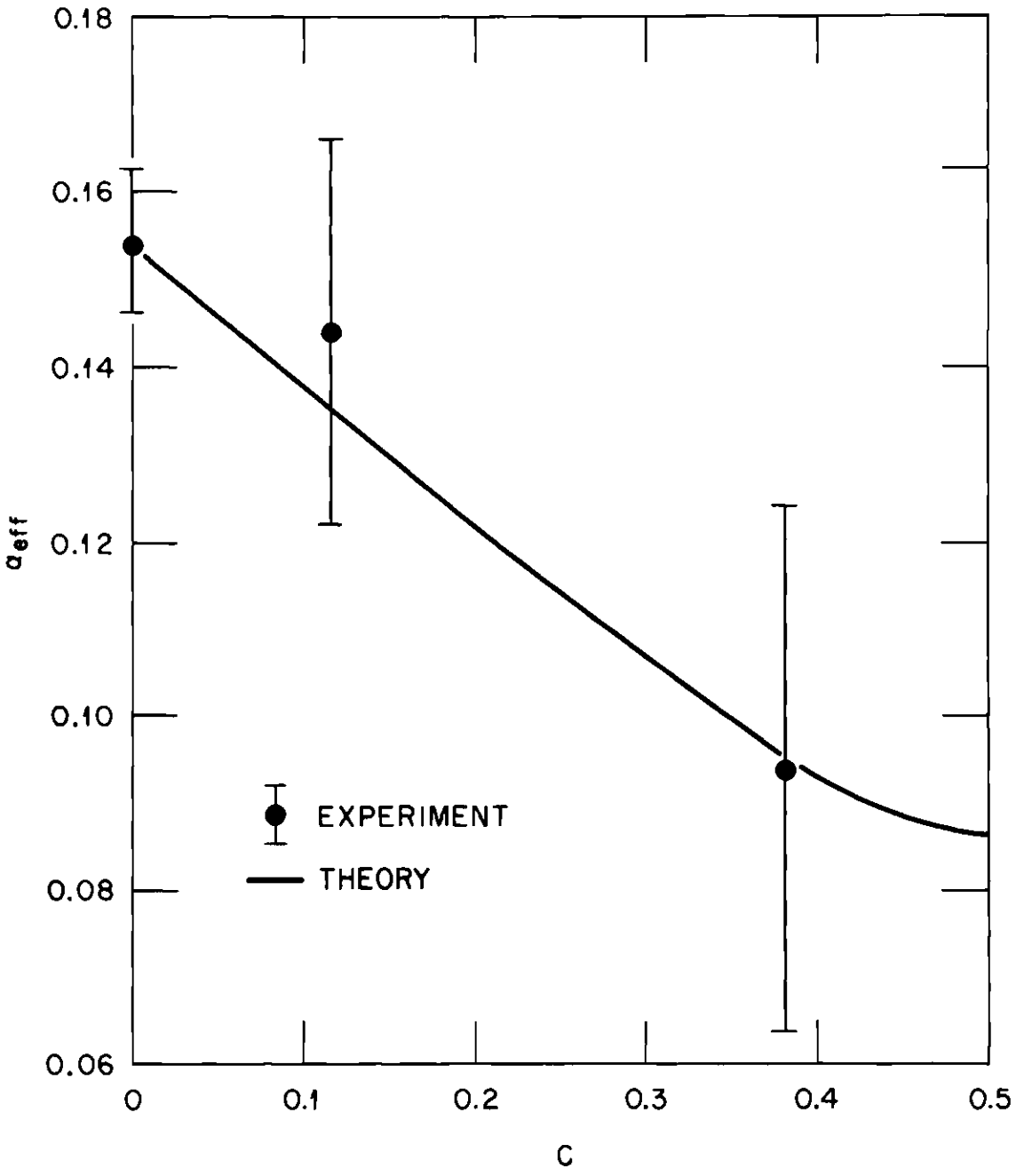

Figure 7. Fraction of Nonlocal Moment in Ni-Cu Alloys

$$M(K)/\langle f(K)\rangle = \sum_{\lambda} Z_{\lambda} m_{\lambda} j_o(KR_{\lambda}). \tag{4}$$

Here Z_λ and R_λ keep the meaning they have in equation (V.1), while the m_λ are the moment disturbances. The fitted values of $m_o = \Delta\langle\mu\rangle = \langle\mu_{Cu}\rangle - \langle\mu_{Ni}\rangle$ are shown in Table 3. For comparison, values of $\langle\mu\rangle/(1-c)$ are also given. The agreement between these two quantities indicates that the Cu moment is essentially zero, as the calculated values in the last column of the table confirm. The low field value of $\langle\mu\rangle$ for the 52.5% alloy was measured by us. All the other values of $\langle\mu\rangle$ and those of $d\langle\mu\rangle/dc$ were obtained from published magnetization data.[21,24,34-38] The second way of analyzing the data is to fit the quantity $M(K)/\left(\langle f(K)\rangle S(K)\right)$ to an expression similar to (V.4). The extrapolation of this quantity to K = 0 gives the values of $M(0)/S(0)$ presented in Table 3. Both fittings and the data are shown in Fig. 8 where the arrows indicate the values of $\frac{d\langle\mu\rangle}{dc}$. Finally, the data are also analyzed with the many-site perturbations expansion in order to extract from them the moment disturbances corresponding to the random alloy. This is done by fitting the data with equation (III.25) to obtain the parameters γ_λ. The one-site perturbations, $\phi_1(r)$, are then calculated using these γ_λ in equation (III.27). As a check of this procedure we have calculated the average Ni moment in the alloy with SRO using equation (III.10). The results of this calculation together with the average Ni moments for the random alloy, $\bar{\mu}_{Ni} = -\phi_1(0)$, and the other $\phi_1(R_\lambda)$ are given in Table 4. For the 52.5% alloy, a tail of the form of a Yukawa potential was assumed in fitting for the shells from the 5th through the 13th neighbors.

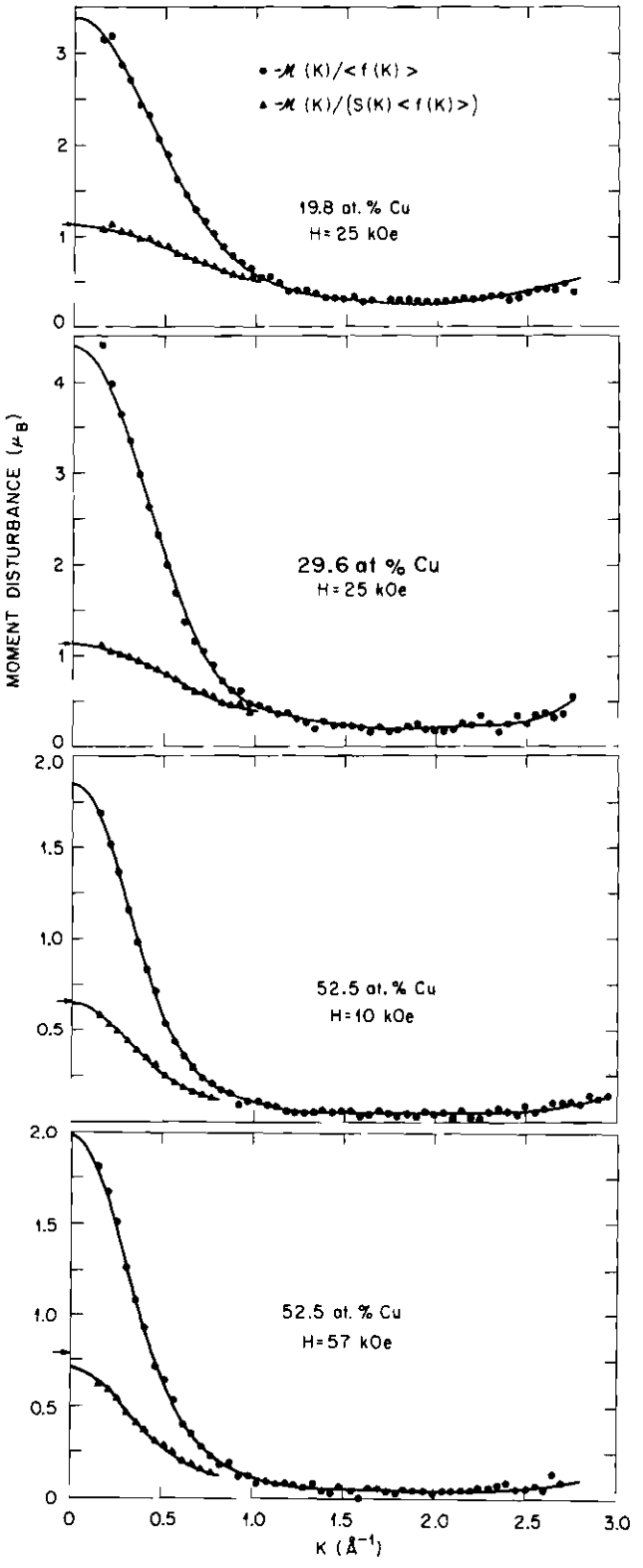

Figure 8. Ni-Cu Polarized Neutron Moment Disturbances

Table 4. Moment Disturbances of Random Ni-Cu Alloys

c	0.198	0.296	0.525	0.525 (HF)
$\langle\mu_{Ni}\rangle_{cal}$	0.481	0.414	0.090	0.106
$\bar{\mu}_{Ni}$	0.466	0.382	0.0765	0.776
$\phi_1(R_1)$	-0.0401	-0.0395	-0.01125	-0.01561
$\phi_1(R_2)$	-0.0088	-0.0095	-0.01111	-0.00762
$\phi_1(R_3)$	-0.0074	-0.0091	-0.00356	-0.00488
$\phi_1(R_4)$	-0.0034	-0.0054	-0.00904	-0.00319
$\phi_1(R_5)$	-	-	-0.00091	-0.00219
$\phi_1(R_6)$	-	-	-0.00080	-0.00159
$\phi_1(R_7)$	-	-	-0.00072	-0.00118
$\phi_1(R_8)$	-	-	-0.00065	-0.00091
$\phi_1(R_9)$	-	-	-0.00060	-0.00071
$\phi_1(R_{10})$	-	-	-0.00055	-0.00056
$\phi_1(R_{11})$	-	-	-0.00051	-0.00045
$\phi_1(R_{12})$	-	-	-0.00048	-0.00037
$\phi_1(R_{13})$	-	-	-0.00045	-0.00031

Comparison with the Unpolarized Neutron Data

Our values of $-\Delta\langle\mu\rangle$ are smaller than those obtained from the unpolarized neutron experiments. For example, at 20% Cu we obtain $\Delta\langle\mu\rangle = -0.478\ \mu_B$ compared with the previous result[20,21] of $-0.60\ \mu_B$. We attribute this discrepancy partially to the previous authors having neglected the difference between the spherical average of a product and the product of the spherical averages in Marshall's expression for the cross section (equivalent to our equation (III.20)). This approximation is correct at small K but wrong for the large K values that are important in determining $\Delta\langle\mu\rangle$. We have reanalyzed the 20 at.% Cu data of Reference 20 using the same form factor of equation (V.2). The moment-moment correlation $T(\underline{K})$ divided by $\langle f(K)\rangle^2$ was fitted to an expression like (V.4) to obtain the K-independent term $\langle(\delta\mu_{\underline{m}})^2\rangle[c(1-c)]^{-1}$. The value we get is $0.36\ \mu_B^2$. This value, together with the average moment for that concentration and equation (II.14), gives the fluctuation of Ni moments, $\langle(\delta\mu_{Ni})^2\rangle = 0.025\ \mu_B^2$. The improper treatment of the spherical average is equivalent to neglecting completely this fluctuation and to the assumption that the K-independent term of $T(K)$ is just $(\Delta\langle\mu\rangle)^2$. The fluctuation can be calculated using equation (E.3) and the linear superposition approximation (III.26). With the moment disturbances obtained from our polarized neutron data, we calculate $\langle(\delta\mu_{Ni})^2\rangle = 0.010\ \mu_B^2$. This value is only half of the observed fluctuations; we attribute the remainder to the many-site disturbances.

To sum up this chapter, the magnetic moments in Ni-Cu, including the "uniform" negative magnetization, are associated with nickel atoms

and there is no contradiction between the diffuse scattering and the diffraction data.

CHAPTER VI

MAGNETIC ENVIRONMENT MODEL

The large moment reductions produced by any nonmagnetic impurity in Ni usually extends to many neighbors. Even Cu, an element for which the charge transfer is expected to be unimportant, produces a long ranged moment disturbance in the concentrated alloys. This suggests that the moment of a nickel atom is a function not only of its nearest chemical environment but also of the magnetic moments of the surrounding atoms, because in this way a mechanism for the long ranged disturbances is established; i.e., the moment reduction produced on its nickel neighbors by the lack of moment on a copper atom is propagated to the neighbors of those neighbors and so on.

Different models incorporating this idea have been proposed.[19,25,39-42] In particular, Hicks[42] proposed a magnetic environment model for Ni-Cu near the critical concentration which is very similar to the one developed here. Our model differs from Hicks in four aspects: (1) it does not assume a particular form for the response function, (2) it is developed for the ferromagnetic instead of the critical region, (3) it allows for a chemical environment effect and (4) we obtain a different analytical solution.

The proposed model is the following: the moment on a nickel atom is assumed to be a function of the number of its Cu neighbors and of an effective exchange field produced by its neighbors. A random alloy is assumed. We have then,

$$\mu_{\underline{m}} = (1-p_{\underline{m}})\ F\left[h(\underline{m}),\ \nu(\underline{m}),\ c\right], \tag{1}$$

in which h is the exchange field given by

$$h(\underline{n}) = \sum_{\underline{m}} j(\underline{n}-\underline{m})\ \mu_{\underline{m}}$$

$$j(0) = 0 \tag{2}$$

and ν is the number of Cu next neighbors (a greek site index will stand for first neighbors).

$$\nu(\underline{m}) = \sum_{\underline{\delta}} p_{\underline{m}} + \underline{\delta} \tag{3}$$

The explicit concentration dependence of F takes into account the chemical environment beyond the first shell.

An approximate solution can be obtained if the equations are linearized in a way similar to that used by Lovesey and Marshall[43] in treating the temperature dependence of the cross section. If we assume that the fluctuations are small and that the chemical environment effect is small, we may write:

$$F\left[h(\underline{n}),\nu(\underline{n}),c\right] \simeq F(h_{eff},\ \langle\nu\rangle,\ c) + \frac{\partial F}{\partial h}\left[h(\underline{n})-h_{eff}\right] + \frac{\partial F}{\partial \nu}\left[\nu(\underline{n})-\langle\nu\rangle\right] \tag{4}$$

where h_{eff} is an effective field defined as:

$$\bar{\mu}_{Ni} = \frac{\bar{\mu}}{1-c} = F(h_{eff},\ \langle\nu\rangle,\ c). \tag{5}$$

By multiplying equation (VI.4) by $(1-p_n)$ and taking the average, one obtains the following equation for the effective field:

$$\langle(1-p_{\underline{n}})\left[h(\underline{n}) - h_{eff}\right]\rangle = 0. \tag{6}$$

It is convenient now to introduce the many-site perturbations of the moment:

$$\mu_{\underline{n}} = \bar{\mu} + \sum_{\underline{r}} \phi_1(\underline{r}-\underline{n})(p_{\underline{r}}-c) + \tfrac{1}{2} \sum_{\underline{r},\underline{t}} \phi_2(\underline{r}-\underline{n},\underline{t}-\underline{n})(p_{\underline{r}}-c)(p_{\underline{t}}-c) + \cdots \tag{7}$$

Insertion of this into the definition of the exchange field gives

$$h(\underline{n}) = \sum_{\underline{m}} j(\underline{n}-\underline{m})\mu_{\underline{m}} = \bar{\mu}\Big(\sum_{\underline{r}} j(\underline{r})\Big) + \sum_{\underline{r}} \sum_{\underline{m}} j(\underline{n}-\underline{m})\phi_1(\underline{r}-\underline{m})(p_{\underline{r}}-c)$$

$$+ \tfrac{1}{2} \sum_{\underline{r},\underline{t}} \Big(\sum_{\underline{m}} j(\underline{n}-\underline{m})\phi_2(\underline{r}-\underline{m},\underline{t}-\underline{m})\Big)(p_{\underline{r}}-c)(p_{\underline{t}}-c) + \cdots \tag{8}$$

which, with (VI.6), yields

$$h_{eff} = \bar{\mu} \sum_{\underline{r}} j(\underline{r}) - c \sum_{\underline{m}} j(\underline{m})\phi_1(\underline{m}). \tag{9}$$

We now obtain an equation for the one-site perturbations $\phi_1(r)$. From equation (VI.7), it follows that

$$c(1-c)\ \phi_1(\underline{r}) = \langle (p_{\underline{r}}-c)\ \mu_o \rangle. \tag{10}$$

from which we obtain $\phi_1(\underline{r})$ by using the expression for the moment given by equations (VI.1) and (VI.4), i.e.,

$$\phi_1(\underline{r}) = -\bar{\mu}_{Ni}\delta_{\underline{r}o} + \frac{\partial F}{\partial h}\ [(1-c)(1-\delta_{\underline{r}o}) \sum_{\underline{m}} j(-\underline{m})\ \phi_1(\underline{r}-\underline{m})$$

$$- c(1-c) \sum_{\underline{n}} j(-\underline{n})\ \phi_2(\underline{r}-\underline{n}, -\underline{n})]$$

$$+ \frac{\partial F}{\partial \nu}\ (1-c) \sum_{\underline{\rho}} \delta_{\underline{\rho}\ \underline{r}}. \tag{11}$$

Note that ϕ_2 appears in this equation. In the same way, we can obtain an equation for ϕ_2 in which ϕ_3 appears. In general, an infinite set of equations can be obtained, each one relating the n-site perturbations

with n+1 site perturbations. One way of solving the problem is to neglect the n+1-site perturbations and to solve the truncated system of equations. We limit ourselves here to the first equation of the infinite set, which means that we neglect the two-site perturbations. This is justified because the average moment decreases linearly with concentration in the region 0-45 at.% Cu, and because the relation (III.20) between polarized and unpolarized neutron cross sections is roughly satisfied for Ni-Cu. Furthermore, when the two-site perturbations are included, the polarized neutron cross section, $\Phi_1(K)$, has approximately the same mathematical form of the cross section obtained taking only the one-site perturbations. Only the values of the parameters are different. We then drop the two-site perturbations and Fourier transform equation (VI.11) to obtain:

$$\Phi_1(\underline{K}) = - \frac{\bar{\mu}_{Ni} + \Gamma \sum_{\underline{n}} j(n)\ \phi_1(\underline{n})/J(0) - \Gamma Z_1 \rho F_1(\underline{K})}{1 - \Gamma J(\underline{K})/J(0)} \qquad (12)$$

Here J and Φ_1 are the Fourier transforms of j and ϕ_1, respectively. We have also introduced

$$\Gamma = \frac{\partial F}{\partial h}\ (1-c)\ J(0) \qquad (13)$$

$$\rho = \frac{\partial F}{\partial \nu}\ (1-c)/\Gamma \qquad (14)$$

$$F_1(\underline{K}) = 1/Z_1 \sum_{\delta} e^{i\underline{K}\cdot\underline{\delta}} \ . \qquad (15)$$

The parameter Γ is related to the range of the one-site perturbations, while ρ measures the strength of the chemical environment effect. The

quantity $\sum_{\underline{n}} j(\underline{n})\phi_1(\underline{n})$ appearing in equation (VI.12) is determined by equation (VI.12) since

$$\sum_{\underline{n}} j(\underline{n})\ \phi_1(\underline{n}) = 1/V_{FBZ} \int_{FBZ} d^3K\ J(\underline{K})\ \Phi_1(\underline{K}). \tag{16}$$

Using (VI.16), we find

$$\frac{1}{J(0)} \sum_{\underline{n}} j(\underline{n})\ \phi_1(\underline{n}) = -\bar{\mu}_{Ni} \frac{B(\Gamma)-1}{B(\Gamma)\Gamma} + \rho Z_1\ \tilde{B}(\Gamma)/B(\Gamma), \tag{17}$$

where $B(\Gamma)$ and $\tilde{B}(\Gamma)$ are defined by

$$B(\Gamma) = 1/V_{FBZ} \int_{FBZ} d^3K\ \frac{1}{1 - \Gamma J(\underline{K})/J(0)} \tag{18}$$

and

$$\tilde{B}(\Gamma) = 1/V_{FBZ} \int_{FBZ} d^3K\ \frac{F_1(\underline{K})}{1 - \Gamma J(\underline{K})/J(0)}\ . \tag{19}$$

The function $B(\Gamma)$ has the same form as a one-electron Green's function. Using (VI.17) in (VI.12) and (VI.9), we find,

$$\Phi_1(\underline{K}) = \frac{-\bar{\mu}_{Ni} + Z_1\rho\ \Gamma\left(B(\Gamma)\ F_1(\underline{K}) - \tilde{B}(\Gamma)\right)}{B(\Gamma)\ \left(1-\Gamma\ J(\underline{K})/J(0)\right)} \tag{20}$$

and

$$h_{eff} = \bar{\mu}_{Ni}\ J(0)\ \left[(1-c) + c\ \frac{B(\Gamma)-1}{B(\Gamma)\Gamma}\right] - c\ J(0)\ Z_1\rho\tilde{B}(\Gamma)/B(\Gamma). \tag{21}$$

When ϕ_2 terms are included, $\Phi_1(\underline{K})$ is still approximately given by equation (VI.20) but with Γ replaced by a different value. We can then treat the effect of the neglected many-site perturbations by considering Γ as a parameter to be determined. Γ then assumes the value given by equation (VI.13) only at zero impurity concentration. The parameter Γ .

can be obtained self-consistently by imposing the equality of $\Phi_1(0)$ and the concentration derivative of the average moment,

$$\frac{d\bar{\mu}}{dc} = \Phi_1(0). \tag{22}$$

This equation, together with (VI.5), (VI.14), (VI.20), and (VI.21), determines Γ and $\bar{\mu}$ as functions of concentration for any given $F(h,\nu,c)$.

In the particular case of nearest-neighbor exchange, the equations assume a simpler form. In this case

$$J(\underline{K}) = J(0)\ F_1(\underline{K}), \tag{23}$$

$$\tilde{B}(\Gamma) = \left[B(\Gamma) - 1\right]/\Gamma, \tag{24}$$

and equation (VI.20) reduces to

$$\Phi_1(\underline{K}) = -\rho Z_1 - \frac{\bar{\mu}_{Ni} - \rho Z_1}{\left[1-\Gamma\ F_1(\underline{K})\right]B(\Gamma)}\ . \tag{25}$$

Furthermore, the function $B(\Gamma)$ has been calculated analytically[44] for nearest neighbor exchange in a fcc lattice; the result is the following combination of complete eliptic integrals:

$$B(\Gamma) = 12\ \pi^{-2}\ (3+\Gamma)^{-1}\ K[k_+(\Gamma)]\ K[k_-(\Gamma)] \tag{26}$$

$$[k_\pm(\Gamma)]^2 = \frac{1}{2} \pm 2\sqrt{3}\ \Gamma\ (3+\Gamma)^{-3/2} - \frac{\sqrt{3}}{2}\ (3-\Gamma)(1-\Gamma)^{1/2}\ (3+\Gamma)^{-3/2} \tag{27}$$

and

$$K(k) = \int_0^{\pi/2} [1 - (k\sin\theta)^2]^{-1/2}\ d\theta. \tag{28}$$

CHAPTER VII

COMPARISON OF THE MAGNETIC ENVIRONMENT MODEL WITH THE DATA

Moment Disturbances

The magnetic environment model of the previous chapter should be compared with the random alloy moment disturbances. The model gives a simple formula for $\Phi_1(\underline{K})$, but not for the coefficients $\phi_1(R)$. It is therefore more convenient to compare the model with a pseudo-experimental $\Phi_1(\underline{K})$ obtained from the $M(\underline{K})$ data by requiring that the percentage difference of the pseudo-data and the calculated $\Phi_1(\underline{K})$ be equal to the percentage difference between the $M(\underline{K})$ data and their fitted values. The $\Phi_1(\underline{K})$ so obtained are shown in Fig. 9. The continuous lines in the figure represent the result of the fitting of the magnetic environment model with nearest-neighbor exchange (formula VI.25) and give a good description of the data. The values of the free parameters $\bar{\mu}_{Ni}$, Γ, and ρ are given in Table 5. The values of $\bar{\mu}_{Ni}$ obtained by the two different fittings are in reasonable agreement (see Tables 4 and 5). The change of the moment disturbances produced by the high field for the 52.5% alloy scales approximately with the change of moment. A small decrease of Γ is also observed. In Table 5 are also given the values of the "chemical environment" part of the first-shell moment disturbance, $\rho\Gamma$. Comparison with the values of $\phi_1(R_1)$ given in Table 4 shows that most of the effect is due to the magnetic environment.

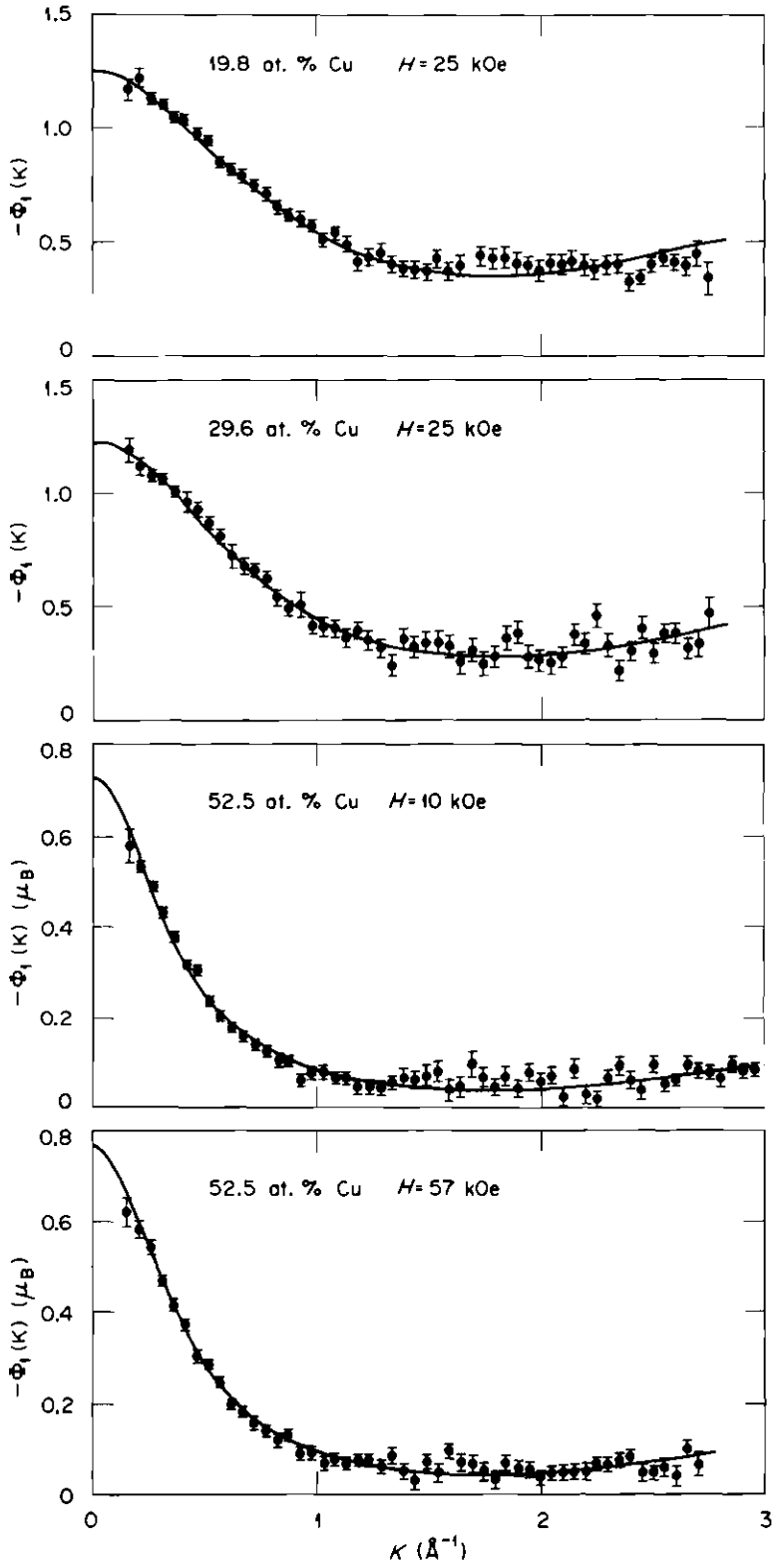

Figure 9. Fitting of Ni-Cu Data with the Magnetic Environment Model

Table 5. Fitting of the Magnetic Environment Model

c	$\overline{\mu}_{Ni}$	Γ	ρ	χ^2/N	$\rho\Gamma$
0.198	0.461 (6)	0.515 (34)	-0.027 (8)	1.23	-0.0139
0.296	0.379 (8)	0.583 (36)	-0.023 (7)	1.15	-0.0135
0.525	0.0713 (29)	0.871 (10)	-0.0034 (7)	1.41	-0.0029
0.525 (HF)	0.0776 (26)	0.856 (9)	-0.0046 (6)	0.98	-0.0039

Response Function

We now present a semi-phenomenological determination of the response function, $F(h,\nu,c)$, that appears in the magnetic environment model. Our purpose is not to give an exact calculation of $F(h,\nu,c)$, but rather to illustrate the behavior of the model. We start by considering the pure Ni case. Cooke and Davis[45] have calculated the bands of ferromagnetic Ni using the paramagnetic band structure of Stocks et al.[17] Their band calculation shows a $\underline{K}$-dependent exchange splitting. However, the integrated density of states they obtain can be approximately described with a different rigid splitting for each one of the t_{2g}, e_g, and sp densities of states. We use the Stocks et al. densities of states of paramagnetic Ni, shown in Fig. 10, for estimating the spin moment as a function of the t_{2g} band half-splitting, I. A variety of splitting schemes were tried and they yield different values between 0.0135 and 0.0160 ry for the splitting, I_o, which reproduces the observed spin moment (0.56 μ_B). However, all of them give almost identical results when the spin moment is plotted against I/I_o. This plot is given in Fig. 11. We assume that this function applies locally to each Ni atom, and that the splitting I is linearly dependent on the moment of the atom itself and on those of the nearest neighbors. We then write the splitting of the atom at site $\underline{r}$ as:

$$I_{\underline{r}} = j_o \mu_{\underline{r}} + j_1 \sum_{\underline{\delta}} \mu_{\underline{r}+\underline{\delta}}$$

$$= j_o \mu_{\underline{r}} + h(\underline{r}) \qquad (1)$$

where j_o is the intraatomic and j_1 is the interatomic exchange parameter.

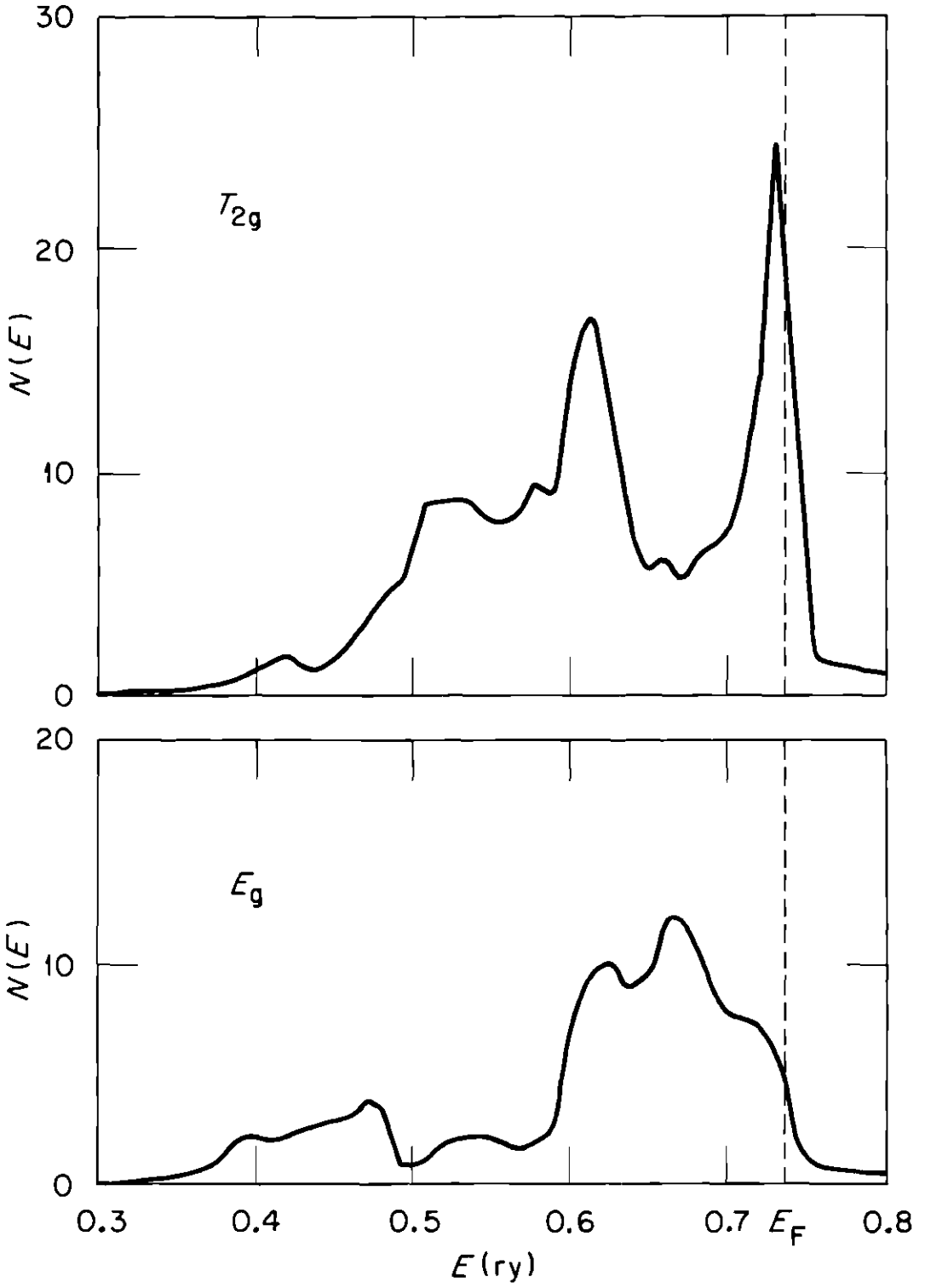

Figure 10. Paramagnetic Ni Densities of States

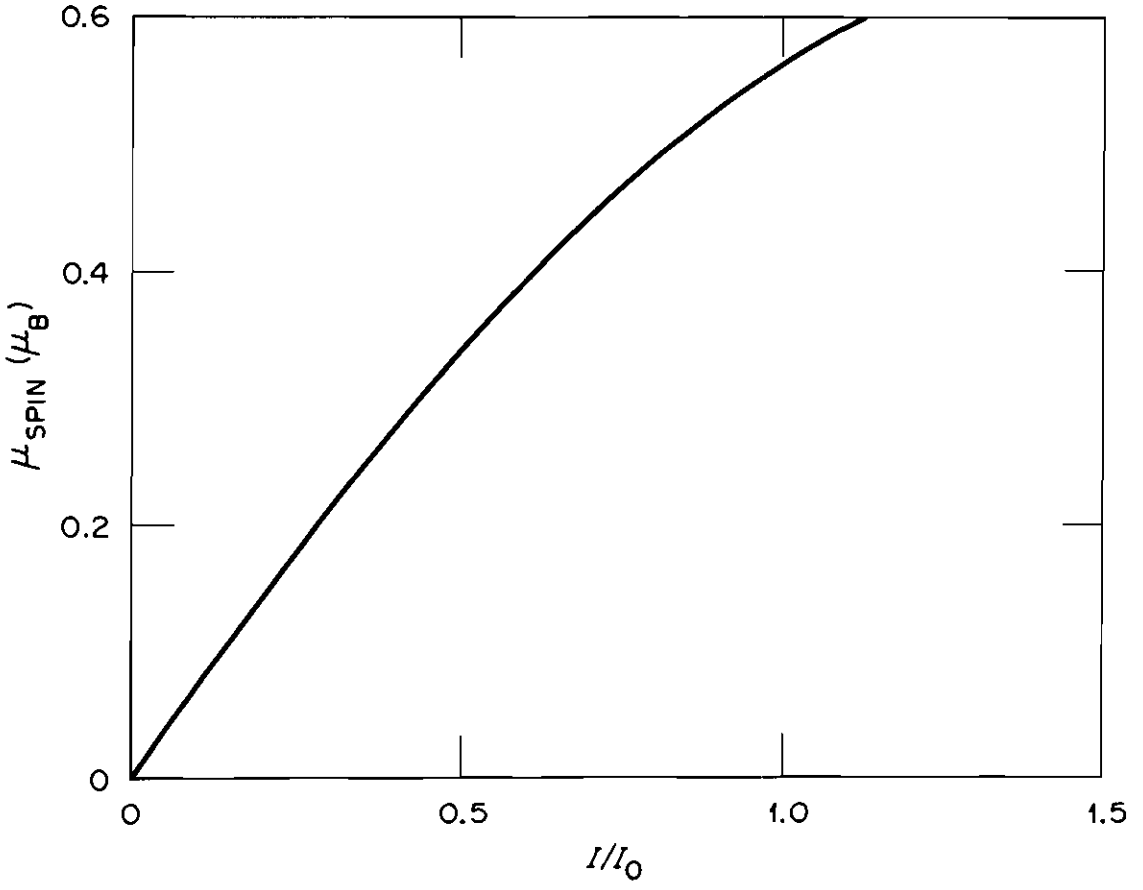

Figure 11. Spin Moment of Ni versus the Relative Band Splitting

We consider now the Ni-Cu case. We use the same procedure to determine the spin moment as a function of splitting for different Cu concentrations, using the Ni densities of states given by the CPA calculations of Ref. 17. The moment-versus-splitting curves so obtained are roughly proportional to the pure Ni curve. However, the decrease of moment predicted using these curves is too large; the predicted critical concentration is less than 40 at.% Cu. Instead of using those functions, we assume the following phenomenological formula for the moment of a Ni atom at site $\underline{r}$ and surrounded by ν Cu atoms.

$$\mu_{\underline{r}} = (1 - \beta\nu)\ g/2\ f(I_{\underline{r}}). \tag{2}$$

Here, $I_{\underline{r}}$ is given by equation (VII.1), β is a parameter that measures the strength of the "chemical environment effect," and $f(I)$ is the spin moment for a splitting I in pure Ni. Equations (VII.2) and (VII.1) give an implicit definition of the response function $F(h,\nu)$. The explicit c dependence is neglected. Equations (VII.2) and (VI.14) give the following expressions for ρ:

$$\rho = -\frac{\beta}{1-12c\beta}\,\frac{\bar{\mu}}{1 - (1-12c\beta)\ g/2\ df/dI\ j_o}\,\frac{1}{\Gamma}\ , \tag{3}$$

and for Γ at zero impurity concentration,

$$\Gamma_o = \frac{12\ j_1\ g/2\ df/dI}{1 - g/2\ df/dI\ j_o}\ . \tag{4}$$

So far we have two unknown parameters, β and α, the fraction of the splitting that is due to interatomic exchange, i.e.,

$$\alpha = \frac{12j_1}{j_o + 12j_1}\ . \tag{5}$$

The self-consistent method explained in the previous chapter gives Γ and $\bar{\mu}$ as a function of Cu content for any given $F(h,\nu,c)$. We use this fact to determine the values of α and β that reproduce the magnetization data. In doing this, we take into account the random alloy assumption by calculating, with equation (III.10), the moment in the presence of clustering. In the calculation only $\alpha(R_1)$ was assumed nonzero. We find the intervals $0.20 < \alpha < 0.40$ and $0.01 < \beta < 0.02$ for the parameters. The values $\alpha = 0.32$ and $\beta = 0.0154$ give the best agreement with the cross sections. The average moment calculated using these values is shown in Fig. 12 while Γ and ρ are given in Fig. 13 together with the experimental values. The 10 at.% and 40 at.% Cu unpolarized neutron data of Aldred et al.[21] are compared with the predicted cross sections in Fig. 14. We see that this very simple model gives the right trend of the cross sections. Some difference is to be expected in the 40% alloy because of the problems of the unpolarized neutron data already discussed in Chapter IV. We do not expect the model to properly describe the critical region, because it completely neglects the appearance of uncoupled superparamagnetic clusters which are polarized when a magnetic field is applied. It has been implicitly assumed instead that all the moments are aligned. The predicted critical concentration is 60 at.% Cu ($\Gamma \sim 1$) which agrees more with the concentration at which the Curie-Weiss interaction temperature goes negative[46] than with the observed critical concentration of 57 at.% Cu. The difficulties in the critical region are due to the particular solution and not to the magnetic environment model itself, which can actually be used for estimating the stability of clusters and their moments in the paramagnetic alloys.

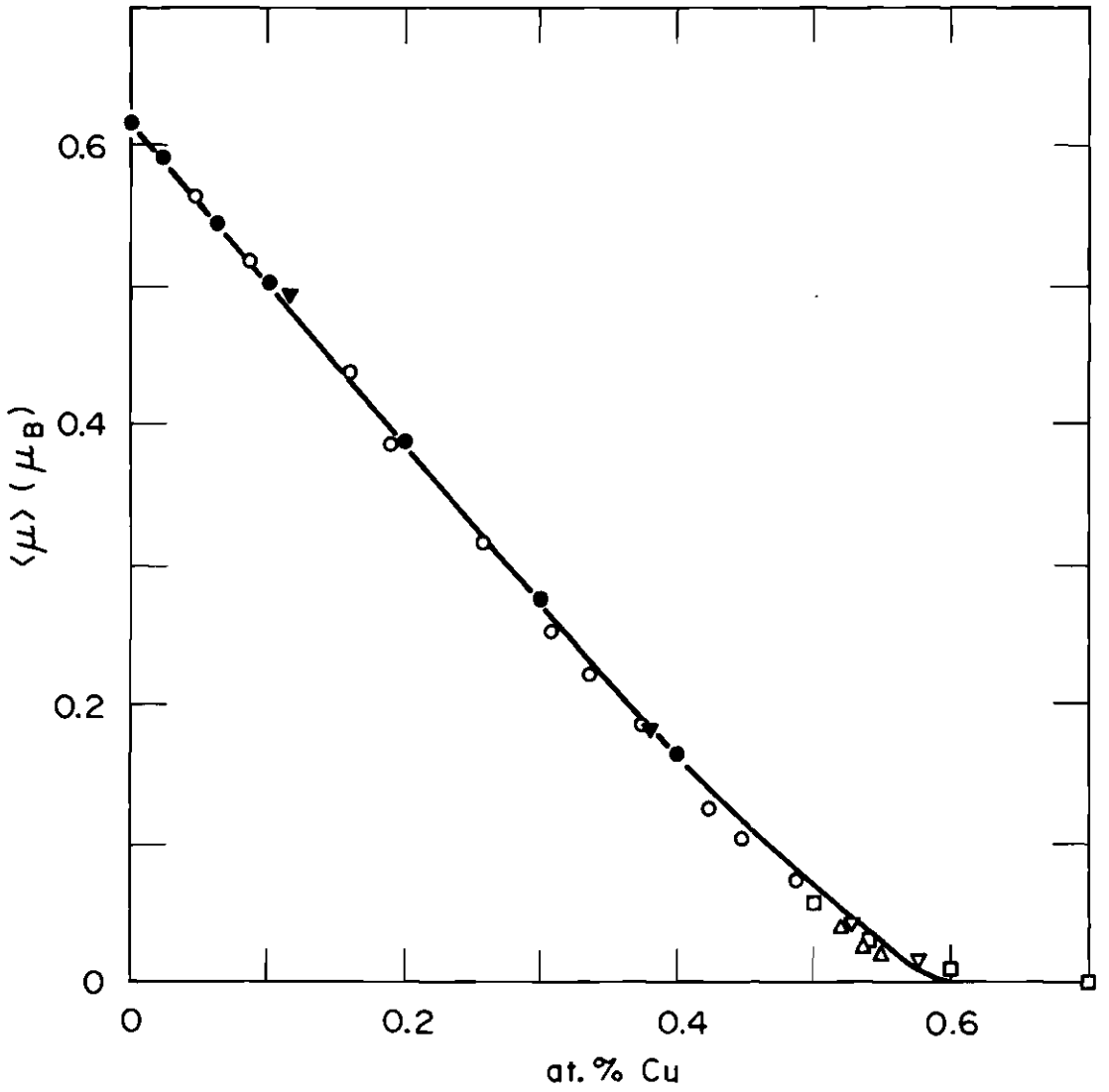

▼Ref. 24, oRef. 34 (normalized to a pure Ni moment of o,616 μ_B), ●Ref. 21, ΔRef. 35, ▽Ref. 36, ■ Ref. 37.

Figure 12. Data and Theoretical Calculation of the Ni-Cu Average Moment

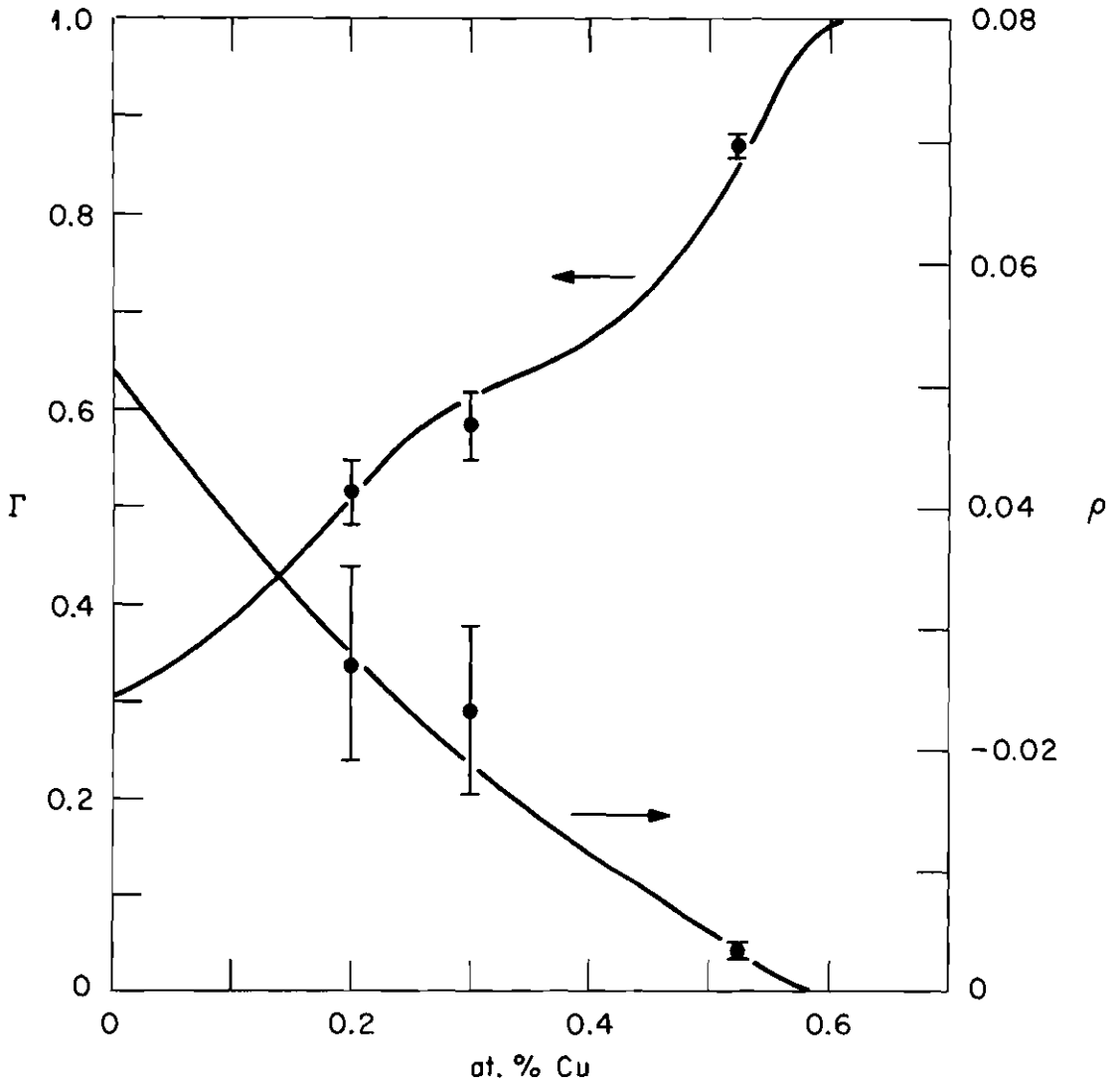

Figure 13. Experimental and Theoretical Values of the Parameters Γ and ρ of the Magnetic Environment Model

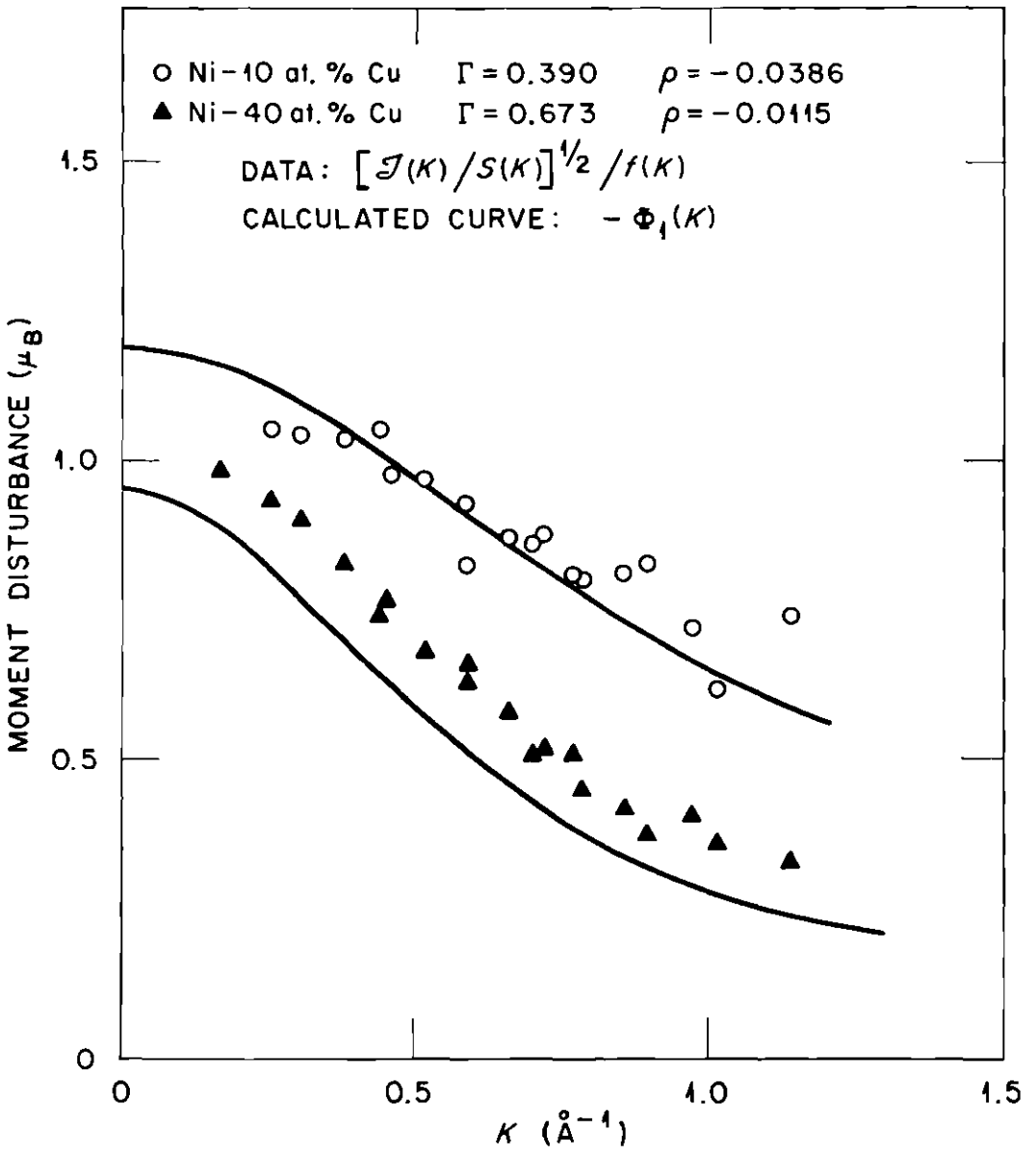

Figure 14. Ni-Cu Unpolarized Neutron Moment Disturbances from Ref. 21 Compared with the Predictions of the Magnetic Environment Model

Dilute Impurities

The value of Γ at zero concentration, Γ_o, is a property of pure Ni. We should therefore expect that any dilute nonmagnetic impurity produces a moment disturbance $\Phi_1(\underline{K})$ described by equation (VI.25) with Γ equal to Γ_o, and a ρ that depends on the strength of the "chemical perturbation." The value of Γ_o calculated with the chosen parameters α and β is $\Gamma_o = 0.305 \pm 0.05$. Using this value we have calculated ρ in the dilute limit for different nonmagnetic impurities by equating $d\langle\mu\rangle/dc$ with $\Phi_1(0)$. When no derivative value was available, we used a Φ_1 value calculated from the data of Ref. 19. The results of this calculation are plotted in Fig.15 and show an increase of the chemical disturbance as the atomic number of the impurity moves away from Ni. As an example, we present in Fig.16 the Ni-1 at.% Cr polarized neutron data of Cable and Medina,[47] and the Ni-Zn data of Comly et al.[19] together with the predicted moment disturbances. The agreement of predicted and measured moment disturbances of impurities as different as Zn and Cr indicates that the Γ_o estimated is not far from the actual value. We should note that the present model, in contrast with the one proposed by Comly et al.,[19] does not predict a universal moment disturbance; the shape of the moment disturbance is instead ρ-dependent. For example, Zn was considered to be anomalous because of the shorter range of its moment disturbance, but this is given correctly by the present model. Their qualitative discussion of the moment perturbation induced by an impurity on its Ni neighbors and its propagation through the nickel matrix is, however, also applicable to our model.

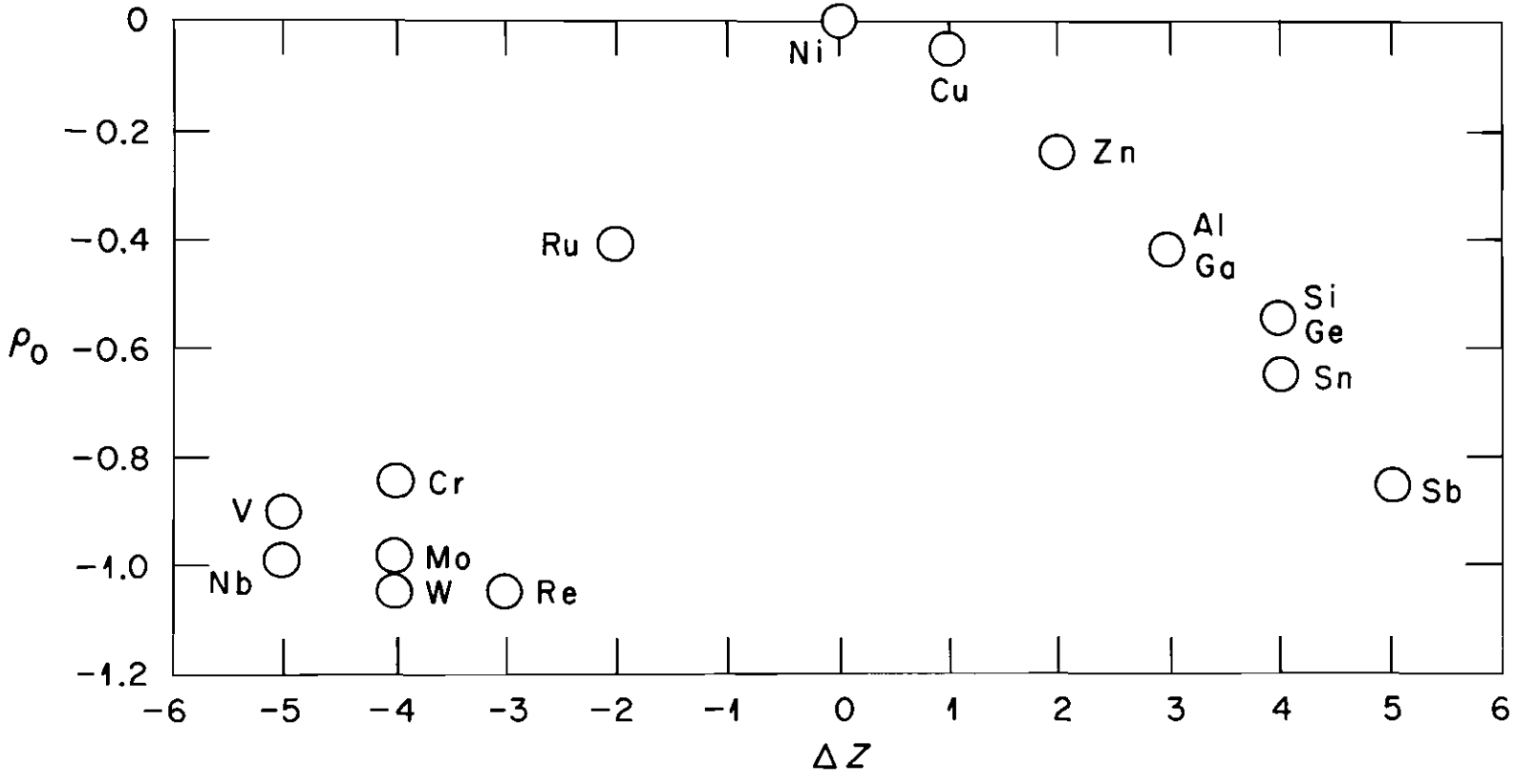

Figure 15. The Chemical Disturbance Parameter ρ for Different Diluents in Ni as a Function of the Charge Contrast

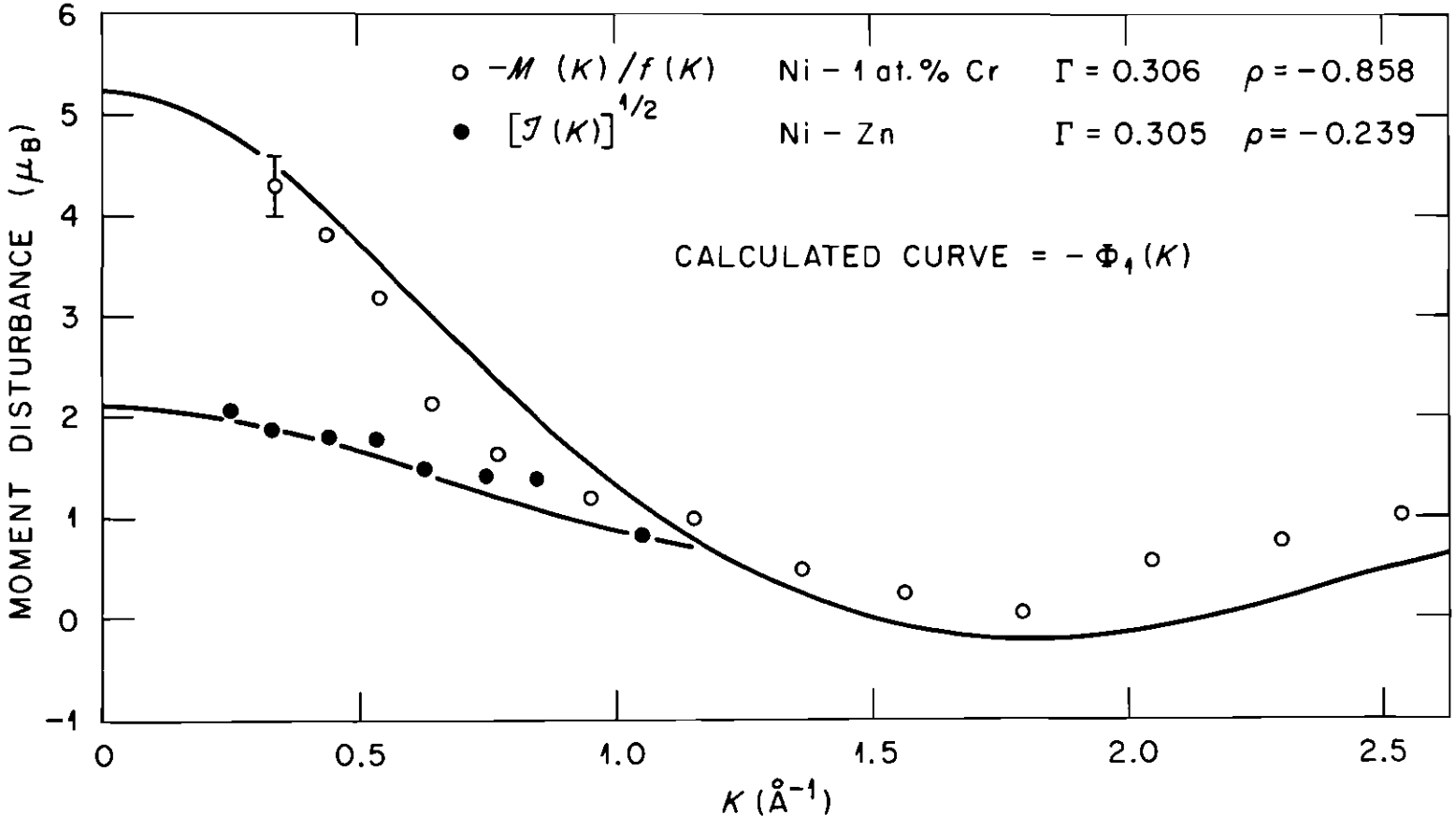

Figure 16. Ni-Cr (1 at. %) Polarized Neutron Data of Ref. 47 and Ni-Zn (between 2 and 4%) Unpolarized Neutron Data of Ref. 19 Compared with the Theoretical Predictions

CHAPTER VIII

SUMMARY AND CONCLUSIONS

We have measured the moment disturbances in three ferromagnetic Ni-Cu alloys with the polarized neutron technique. The data indicate that all the magnetic moment, including the negative magnetization previously assumed uniform, is to be associated with the Ni atoms. This agrees with the diffraction data[24] and with the theoretical[16,17] and experimental[14,15] evidence that the Cu atoms keep their 3d shell almost full.

The proposed nearest-neighbor magnetic environment model gives an excellent description of the observed moment disturbances. Within the model one finds that most of the moment disturbances produced by Cu in Ni are due to its nonmagnetic character, but that some nearest neighbor chemical disturbance must be included to explain the observed cross sections. In contrast, none of the first and second shell chemical environment models, like those of references 24, 36, 37, and 48, is consistent with the diffuse scattering data. The proposed model also describes the diffuse scattering of other nonmagnetic dilute impurities in Ni, because the moment disturbance induced by the impurity in its Ni neighbors is propagated through the lattice with the same mechanism, regardless of the origin and size of the disturbance.

The large and long-range moment disturbances produced by impurities suggest that some type of effective interatomic exchange is very important

for Ni. A rough Stoner type of calculation shows that between 20 and 40% interatomic exchange is needed to reproduce the Ni-Cu data. Within the same calculation each Cu atom induces a 1-2% moment reduction on its Ni neighbors for any given exchange field. For a better determination and understanding of these effects, a more accurate and less phenomenological calculation should be performed. However, our data indicate that, independent of the specific model used to describe magnetic cooperative effects, such effects are dominant in determining the magnetic moments in Ni-Cu alloys.

APPENDIX A

Marshall[18] has proved an approximate relationship between the concentration derivative of the average magnetic moment and the unpolarized neutron diffuse scattering in the forward direction. We prove a similar but exact relationship for the polarized neutron cross section as a particular case of a general relationship between concentration derivatives and fluctuations.

The system under consideration is a single crystal of substitutional binary alloy with N lattice sites $\{\underline{r}\}$. The configuration of the sample is determined by the set of occupation numbers $\{p_{\underline{r}}\}$. A probability distribution of configurations consistent with the microscopic properties of the sample can be introduced using the grand canonical ensemble. That is, the sample under consideration is thought of as an element of an ensemble of samples with identical lattices, each one being a small part of some bigger, macroscopically homogeneous crystal. The difference between the values of any quantity in two different crystals of the ensemble is very small. It is then possible to replace the space average in the sample with the average in the configurational ensemble ($\langle\cdots\rangle$).

In the following any configuration dependent quantity, as $p_{\underline{r}}$, will be called an operator in order to differentiate it from the configuration independent quantities such as the number of sites N or any physical quantity of the bigger crystal. More precisely, if y is some intensive physical quantity of the bigger crystal, the corresponding operator for the sample will be denoted by $\hat{y}$ and in general we have,

$$\langle \hat{y} \rangle = y \tag{1}$$

but

$$\langle (\hat{y}-y)^2 \rangle = \langle (\delta\hat{y})^2 \rangle \sim 1/N \ . \tag{2}$$

In particular, the impurity concentration operator is:

$$\hat{c} = \frac{1}{N} \sum_{\underline{n}} p_{\underline{n}}, \tag{3}$$

and we have

$$\langle \hat{c} \rangle = \langle p_{\underline{n}} \rangle = c \tag{4}$$

where c is the concentration in the bigger crystal. The average square fluctuation of concentration is given by

$$\langle (\delta\hat{c})^2 \rangle = \frac{1}{N^2} \sum_{\underline{r},\underline{t}} \langle (p_{\underline{r}}-c)(p_{\underline{t}}-c) \rangle \tag{5}$$

which in general is not zero. Using the definitions of the SRO parameters (II.4) and their Fourier transforms (II.7) one obtains

$$\langle (\delta\hat{c})^2 \rangle = c(1-c)S(0)/N. \tag{6}$$

In general any quantity y is a function of c and the SRO. We can write to first order in the fluctuations

$$\delta\hat{y} = \frac{dy}{dc} \delta\hat{c} + \delta\hat{y}_{SRO}. \tag{7}$$

It is always possible to define SRO parameters that are statistically independent of concentration, so that the fluctuation of y due to SRO fluctuations, $\delta\hat{y}_{SRO}$, satisfies the condition:

$$\langle \delta\hat{y} \ \delta\hat{y}_{SRO} \rangle = 0 \ . \tag{8}$$

This implies that the average of $\delta\hat{y}_{SRO}$ under the condition $\delta\hat{c} = \delta c$ vanishes, i.e. the coefficient of $\delta\hat{c}$ in (A.7) coincides with the concentration derivative as defined operationally. Multiplying the equation (A.7) by $\delta\hat{c}$ and taking the average one gets

$$\langle\hat{y}\delta\hat{c}\rangle = \langle\delta\hat{y}\delta\hat{c}\rangle = \frac{dy}{dc}\langle(\delta\hat{c})^2\rangle, \tag{9}$$

which gives, together with equation (A.6), the general relationship

$$\frac{dy}{dc} = \frac{N\langle\hat{y}\delta\hat{c}\rangle}{c(1-c)\ S(0)}\ . \tag{10}$$

For the proof of (II.15), we need to replace $\hat{y}$ by the average moment operator

$$\hat{\mu} = \frac{1}{N}\sum_{\underline{n}}\mu_{\underline{n}}. \tag{11}$$

The correlation is then

$$\begin{aligned}\langle\hat{\mu}\delta\hat{c}\rangle &= \frac{1}{N^2}\sum_{\underline{n}\,\underline{m}}\langle\mu_{\underline{n}}(p_{\underline{m}}-c)\rangle \\ &= \frac{1}{N}\sum_{\underline{m}}\langle\mu_o(p_{\underline{m}}-c)\rangle \\ &= \frac{c(1-c)}{N}M(0).\end{aligned} \tag{12}$$

Substitution of (A.12) in (A.10) gives

$$\frac{d\langle\mu\rangle}{dc} = M(0)/S(0). \tag{13}$$

APPENDIX B

The moment disturbance parameters introduced in Chapter III allow a convenient way of expressing the cross sections. On the other hand, the parameters used by Balcar and Marshall[26] have a more direct physical meaning. They expand the moment of a host atom at site $\underline{n}$ as:

$$\mu_{\underline{n}}^{h} = \bar{\mu}_h + \sum_{\underline{r}} g(\underline{r})(p_{\underline{n}+\underline{r}}-c) + \sum_{\underline{r},\underline{t}} a(\underline{r},\underline{t})(p_{\underline{n}+\underline{r}}-c)(p_{\underline{n}+\underline{t}}-c) \tag{1}$$

and the moment of an impurity atom as:

$$\mu_{\underline{n}}^{i} = \bar{\mu}_i + \sum_{\underline{r}} h(\underline{r})(p_{\underline{n}+\underline{r}}-c) + \sum_{\underline{r},\underline{t}} b(\underline{r},\underline{t})(p_{\underline{n}+\underline{r}}-c)(p_{\underline{n}+\underline{t}}-c). \tag{2}$$

The parameters g, h, a and b vanish if any of the arguments vanishes. Neglecting the environmental dependence of the form factors, one may write

$$\mu_{\underline{n}}(\underline{K}) = (1-p_{\underline{n}})\ f_h(\underline{K})\mu_{\underline{n}}^{h} + p_{\underline{n}}\ f_i(\underline{K})\mu_{\underline{n}}^{i}. \tag{3}$$

Substituting the expansions (B.1) and (B.2) for the impurity and host moments, one obtains the parameters of Chapter III in terms of Marshall's parameters

$$\bar{\mu}(\underline{K}) = (1-c)\ f_h(\underline{K})\ \bar{\mu}_h + c\ f_i(\underline{K})\bar{\mu}_i, \tag{4}$$

$$\psi_1(\underline{K};\underline{r}) = (1-c)f_h(\underline{K})g(\underline{r}) + c\ f_i(\underline{K})h(\underline{r}) + [f_i(\underline{K})\bar{\mu}_i - f_h(\underline{K})\bar{\mu}_h]\delta_{\underline{r}0}, \tag{5}$$

and finally

$$\psi_2(\underline{K};\underline{r},\underline{t}) = 2(1-c)\ f_h(\underline{K})\ a(\underline{r},\underline{t}) + 2c\ f_i(\underline{K})b(\underline{r},\underline{t})$$

$$+ \delta_{\underline{t}0}[f_i(\underline{K})\ h(\underline{r}) - f_h(\underline{K})g(\underline{r})]$$

$$+ \delta_{\underline{r}0}[f_i(\underline{K})\ h(\underline{t}) - f_h(\underline{K})g(\underline{t})]. \qquad (6)$$

APPENDIX C

Here we prove the relationship (III.9). For simplicity we limit ourselves to the case of n = 2. The general case can be easily proved by induction using the same technique. For the random alloy, equation (II.15) reduces to

$$\frac{d\langle\mu\rangle}{dc} = \Psi_1(0). \tag{1}$$

We need only to define the operator $\hat{\Psi}_1(0)$ and apply the general formula (A.10). The expression for the operator is:

$$\hat{\Psi}_1(0) = [\hat{c}(1-\hat{c})N]^{-1} \sum_{\underline{n}\,\underline{m}} (p_{\underline{n}}-\hat{c})\ \mu_{\underline{m}}. \tag{2}$$

To calculate the correlation, we first replace $\hat{c}$ by $c + \delta\hat{c}$ and expand up to first order in the fluctuation;

$$\hat{\Psi}_1(0) = [c(1-c)N]^{-1} \sum_{\underline{n}\,\underline{m}} (p_{\underline{n}}-c)\mu_{\underline{m}} - \frac{1-2c}{c(1-c)} \Psi_1(0)\delta\hat{c}$$

$$- \frac{N\langle\mu\rangle}{c(1-c)} \delta\hat{c}\ . \tag{3}$$

We then multiply by $\delta\hat{c}$ and take the average to obtain

$$\langle\hat{\Psi}_1(0)\delta\hat{c}\rangle = [c(1-c)N]^{-1} \sum_{\underline{r}\,\underline{t}} \langle(p_{\underline{r}}-c)(p_{\underline{t}}-c)\mu_{\underline{o}}\rangle$$

$$- \frac{\langle(\delta\hat{c})^2\rangle}{c(1-c)} [(1-2c)\,\Psi_1(0) + N\langle\mu\rangle]$$

$$= [c(1-c)N]^{-1} \sum_{\substack{\underline{r}\,\underline{t} \\ \underline{r}\neq\underline{t}}} \langle(p_{\underline{r}}-c)(p_{\underline{t}}-c)\mu_{\underline{o}}\rangle = \frac{c(1-c)}{N} \sum_{\underline{r}\,\underline{t}} \psi_2(0;\underline{r},\underline{t}). \tag{4}$$

Here, we have made use of the identity

$$(p_{\underline{r}}-c)^2 = (1-2c)(p_{\underline{r}}-c) + c(1-c). \tag{5}$$

Substitution of (C.4) into (A.10) yields

$$\frac{d\Psi_1(0)}{dc} = \frac{d^2<\mu>}{dc^2} = \sum_{\underline{r},\underline{t}} \psi_2(0;\underline{r},\underline{t}) = \sum_{\underline{r}} \Psi_2(0;\underline{r}). \tag{6}$$

APPENDIX D

In the case of chemical clustering induced in a system in thermal equilibrium by pairwise forces, the SRO parameters $\alpha(\underline{n})$ ($n\neq 0$) are approximately proportional to $c(1-c)$,[49] and therefore the sum rule of (III.13) assumes the simpler form

$$\sum_{\underline{m}} \eta(\underline{n},\underline{m}) = 2(1-\delta_{\underline{n}\,\underline{o}})(1-2c)(S(0)-1)\alpha(\underline{n}). \tag{1}$$

On the other hand, the sum of three-site SRO parameters that appears in the definition of $U(\underline{K})$ (III.17) can be rewritten in the form

$$\sum_{\underline{n}} e^{i\underline{K}\cdot\underline{n}}\,\eta(\underline{r}-\underline{n},\underline{t}-\underline{n}) = \sum_{\underline{n}} e^{i\underline{K}\cdot\underline{n}}\,\eta(\underline{r}-\underline{t},\underline{n}-\underline{t})$$

$$= e^{i\underline{K}\cdot\underline{t}} \sum_{\underline{m}} e^{i\underline{K}\cdot\underline{m}}\,\eta(\underline{r}-\underline{t},\underline{m}) \tag{2}$$

which is similar to the left side of (D.1) when $\underline{K} = 0$. This suggests the approximation

$$\sum_{\underline{n}} e^{i\underline{K}\cdot\underline{n}}\,\eta(\underline{r}-\underline{n},\underline{t}-\underline{n}) \simeq (1-2c)(1-\delta_{\underline{r}\,\underline{t}})(e^{i\underline{K}\cdot\underline{t}} + e^{i\underline{K}\cdot\underline{r}})(S(\underline{K})-1)\alpha(\underline{r}-\underline{t}). \tag{3}$$

which is symmetric in $\underline{t}$ and $\underline{r}$ and behaves properly for small values of $\underline{K}$. This approximation, together with (III.17), gives immediately

$$U(\underline{K}) \simeq (1-2c)(S(\underline{K})-1)V(\underline{K}). \tag{4}$$

APPENDIX E

In the presence of SRO, equation (III.3) does not hold. It is, however, convenient to use that equation for defining new many-site disturbances, $\tilde{\psi}_\alpha$, in the presence of SRO

$$\tilde{\psi}_\alpha(\underline{K};\underline{r}_1,\cdots,\underline{r}_\alpha) = [c(1-c)]^{-1} \prod_{\lambda,\nu=1}^{\alpha} [1-(1-\delta_{\lambda\nu})\delta_{\underline{r}_\lambda \underline{r}_\nu}]$$

$$\times \langle (p_{\underline{r}_1}-c)\cdots(p_{\underline{r}_\alpha}-c)(\mu_{\underline{o}}(\underline{K})-\langle\mu(\underline{K})\rangle)\rangle \qquad (1)$$

For the random alloy, the $\tilde{\psi}_\alpha$ are proportional to the ψ_α

$$\tilde{\psi}_\alpha \to [c(1-c)]^{\alpha-1}\ \psi_\alpha. \qquad (2)$$

With the same method used in deriving (III.7) one obtains, in the presence of SRO,

$$\langle \mu_{\underline{m}}(\underline{K})\mu_{\underline{o}}(\underline{K})\rangle = \langle\mu(\underline{K})\rangle^2 + c(1-c) \sum_{\underline{r}} \tilde{\psi}_1(\underline{K};\underline{r})\ \psi_1(\underline{K};\underline{r}+\underline{m})$$

$$+ \frac{c(1-c)}{2!} \sum_{\underline{r},\underline{t}} \tilde{\psi}_2(\underline{K};\underline{r},\underline{t})\ \psi_2(\underline{K};\underline{r}+\underline{m},\underline{t}+\underline{m})$$

$$+ \frac{c(1-c)}{3!} \sum_{\underline{r},\underline{t},\underline{n}} \tilde{\psi}_3(\underline{K};\underline{r},\underline{t},\underline{n})\ \psi_3(\underline{K};\underline{r}+\underline{m},\underline{t}+\underline{m},\underline{n}+\underline{m}) + \cdots \qquad (3)$$

The Fourier transform of this equation gives the unpolarized neutron cross section

$$T(\underline{K}) = \tilde{\Psi}_1(-\underline{K})\ \Psi_1(\underline{K}) + \frac{1}{2!} \sum_{\underline{r}} \tilde{\Psi}_2(-\underline{K};\underline{r})\ \Psi_2(\underline{K};\underline{r})$$

$$+ \frac{1}{3!} \sum_{\underline{r},\underline{t}} \tilde{\Psi}_3(-\underline{K};\underline{r},\underline{t})\ \Psi_3(\underline{K};\underline{r},\underline{t}) + \cdots \qquad (4)$$

Note that this equation contains both the random alloy moment disturbances and the actual moment disturbances; therefore, in order to make use of it, one has to express one kind of disturbance in terms of the other. The one-site disturbances $\tilde{\psi}_1$ have already been calculated in equation (III.14). By definition, it is obvious that

$$M(\underline{K}) = \tilde{\psi}_1(\underline{K}) \ . \tag{5}$$

We now calculate $T(\underline{K})$ neglecting the terms with three-site perturbations. From (III.1) and (III.10), one gets:

$$\mu_{\underline{o}}(\underline{K}) - \langle\mu(\underline{K})\rangle = \sum_{\underline{r}} \psi_1(\underline{K};\underline{r})(p_{\underline{r}}-c) + \frac{1}{2!} \sum_{\underline{r},\underline{t}} \psi_2(\underline{K};\underline{r},\underline{t})(p_{\underline{r}}-c)(p_{\underline{t}}-c)$$
$$- \frac{c(c-1)}{2!} \sum_{\underline{r},\underline{t}} \psi_2(\underline{K};\underline{r},\underline{t})\ \alpha(\underline{r},\underline{t}) \tag{6}$$

from which we obtain, for $\underline{n} \neq \underline{m}$,

$$c(1-c)\ \tilde{\psi}_2(\underline{K};\underline{n},\underline{m}) = \langle(p_{\underline{n}}-c)(p_{\underline{m}}-c)(\mu_{\underline{o}}(\underline{K}) - \langle\mu(K)\rangle)\rangle$$
$$= \sum_{\underline{r}} \psi_1(\underline{K};\underline{r})\ \langle(p_{\underline{r}}-c)(p_{\underline{n}}-c)(p_{\underline{m}}-c)\rangle$$
$$+ \frac{1}{2!} \sum_{\underline{r},\underline{t}} \psi_2(\underline{K};\underline{r},\underline{t})\ \langle(p_{\underline{r}}-c)(p_{\underline{t}}-c)(p_{\underline{n}}-c)(p_{\underline{m}}-c)\rangle$$
$$- \frac{c^2(1-c)^2}{2!} \sum_{\underline{r},\underline{t}} \psi_2(\underline{K};\underline{r},\underline{t})\ \alpha(\underline{r}-\underline{t})\ \alpha(\underline{n}-\underline{m}) \ . \tag{7}$$

Here, we introduce the four-site SRO parameters

$$\eta(\underline{n},\underline{m},\underline{r}) = \begin{cases} = [c(1-c)]^{-2}\ \langle(p_{\underline{n}}-c)(p_{\underline{m}}-c)(p_{\underline{r}}-c)(p_{\underline{o}}-c)\rangle \\ \quad \text{if all site indices are different} \\ = 0 \text{ otherwise.} \end{cases} \tag{8}$$

After some rearrangement of terms, one obtains from (E.7)

$$\tilde{\psi}_2(\underline{K};\underline{n},\underline{m}) = (1-2c)\alpha(\underline{n}-\underline{m})[\psi_1(\underline{K};\underline{n}) + \psi_1(\underline{K};\underline{m})]$$

$$+ \sum_{\underline{r}} \psi_1(\underline{K};\underline{r})\ \eta(\underline{n}-\underline{r},\underline{m}-\underline{r})$$

$$+ \psi_2(\underline{K};\underline{n},\underline{m})[c(1-c) + (1-2c)^2\alpha(\underline{n}-\underline{m}) - c(1-c)\alpha(\underline{n}-\underline{m})^2]$$

$$+ \sum_{\substack{\underline{r} \\ \neq \underline{m}}} \psi_2(\underline{K};\underline{r},\underline{n})[c(1-c)\alpha(\underline{m}-\underline{r}) - c(1-c)\alpha(\underline{n}-\underline{r})\alpha(\underline{n}-\underline{m}) + (1-2c)\eta(\underline{n}-\underline{r},\underline{m}-\underline{r})]$$

$$+ \sum_{\substack{\underline{r} \\ \neq \underline{n}}} \psi_2(\underline{K};\underline{r},\underline{m})[c(1-c)\alpha(\underline{n}-\underline{r}) - c(1-c)\alpha(\underline{m}-\underline{r})\alpha(\underline{n}-\underline{m}) + (1-2c)\eta(\underline{n}-\underline{r},\underline{m}-\underline{r})]$$

$$+ \frac{c(1-c)}{2!} \sum_{\substack{\underline{r},\underline{t} \\ \neq \underline{n},\underline{m}}} \psi_2(\underline{K};\underline{r},\underline{t})[\eta(\underline{n}-\underline{r},\underline{m}-\underline{r},\underline{t}-\underline{r}) - \alpha(\underline{r}-\underline{t})\alpha(\underline{n}-\underline{m})]. \qquad (9)$$

We can now calculate the 2nd term of expansion (E.4). We obtain:

$$\frac{1}{2}\sum_{\underline{r}} \tilde{\Psi}_2(-\underline{K};\underline{r})\ \Psi_2(\underline{K};\underline{r}) = \Psi_1(-\underline{K})[(1-2c)\ V(\underline{K}) + U(\underline{K})]$$

$$+ \frac{1}{2}\sum_{\underline{r}} |\Psi_2(\underline{K};\underline{r})|^2[c(1-c) + (1-2c)^2\alpha(\underline{r}) - c(1-c)\alpha(\underline{r})^2]$$

$$+ \frac{1}{2}\sum_{\underline{r}} [C(-\underline{K},\underline{r}) + C(-\underline{K},-\underline{r})\ e^{i\underline{K}\cdot\underline{r}}]\ \Psi_2(\underline{K};\underline{r})$$

$$+ \frac{c(1-c)}{2} \sum_{\underline{r}} D(-\underline{K},\underline{r})\ \Psi_2(\underline{K};\underline{r}) \qquad (10)$$

where $C(\underline{K},\underline{r})$ is given by

$$C(\underline{K},\underline{r}) = \sum_{\underline{n}} e^{i\underline{K}\cdot\underline{n}} \sum_{\underline{t}\neq\underline{n}+\underline{r}} \psi_2(\underline{K};\underline{t},\underline{n})[c(1-c)\alpha(\underline{n}+\underline{r}-\underline{t})$$

$$- c(1-c)\alpha(\underline{n}-\underline{t})\alpha(\underline{n}) + (1-2c)\eta(\underline{n}-\underline{t},\underline{n}+\underline{r}-\underline{t})] \qquad (11)$$

and

$$D(\underline{K},\underline{r}) = \frac{1}{2} \sum_{\underline{n}} e^{i\underline{K}\cdot\underline{n}} \sum_{\substack{\underline{j},\underline{t} \\ \neq \underline{n},\underline{n}+\underline{r}}} \psi_2(\underline{K};\underline{j},\underline{t})[\eta(\underline{n}-\underline{j},\underline{n}+\underline{r}-\underline{j},\underline{t}-\underline{j})-\alpha(\underline{t}-\underline{j})\alpha(\underline{r})]. \quad (12)$$

Taking only the terms of equation (E.10) linear in ψ_2 and combining with the first term of (E.4), as calculated with (III.15), one obtains

$$T(\underline{K}) \simeq S(K) \; |\Psi_1(\underline{K})|^2 + \Psi_1(-\underline{K})[(1-2c)\; V(\underline{K}) + U(\underline{K})]$$

$$+ [(1-2c)\; V(-\underline{K}) + U(-\underline{K})]\; \Psi_1(\underline{K}) + \cdots \quad (13)$$

Finally, with the approximation (III.18) and neglecting again terms in ψ_2^2, one obtains

$$T(\underline{K}) = S(\underline{K})\; [\Psi_1(\underline{K}) + (1-2c)\; V(\underline{K})]^2 + \cdots \quad (14)$$

REFERENCES

1. C. Sadron, Ann. de Phys. XVII, 371 (1932).

2. E. C. Stoner, Phil. Mag. 15, 1018 (1933).

3. N. F. Mott, Proc. Phys. Soc. 47, 571 (1935).

4. J. C. Slater, J. Appl. Phys. 8, 385 (1937).

5. L. Pauling, Phys. Rev. 54, 899 (1938).

6. E. P. Wohlfarth, Phil. Mag. 40, 703 and 1095 (1949).

7. C. G. Shull and M. K. Wilkinson, Phys. Rev. 97, 304 (1955).

8. J. W. Cable, E. O. Wollan, W. C. Koehler, and M. K. Wilkinson, J. Appl. Phys. Suppl. 33, 1340 (1962).

9. M. F. Collins and D. A. Wheeler, Proc. Phys. Soc. 82, 633 (1963).

10. M. F. Collins and J. B. Forsyth, Phil. Mag. 8, 401 (1963).

11. A. Arrott, M. F. Collins, T. M. Holden, G. G. Low, and R. J. Nathans, J. Appl. Phys. Suppl. 37, 1194 (1966).

12. N. D. Lang and H. Ehrenreich, Phys. Rev. 168, 605 (1968).

13. S. Kirkpatrick, B. Velicky, N. D. Lang, and H. Ehrenreich, J. Appl. Phys. 40, 1283 (1969).

14. D. H. Seib and W. E. Spicer, Phys. Rev. B 2, 1676 and 1694 (1970).

15. S. Hüfner, G. K. Wertheim, R. L. Cohen, and J. H. Wernick, Phys. Rev. Lett. 28, 488 (1972).

16. S. Kirkpatrick, B. Velicky, and H. Ehrenreich, Phys. Rev. B 1, 3250 (1970).

17. G. M. Stocks, R. W. Williams and J. S. Faulkner, Phys. Rev. B 4, 4390 (1971).

18. W. Marshall, J. Phys. C 1, 88 (1968).

19. J. B. Comly, T. M. Holden, and G. G. Low, J. Phys. C 1, 458 (1968).

20. J. W. Cable, E. O. Wollan, and H. R. Child, Phys. Rev. Lett. 22, 1256 (1969).

21. A. T. Aldred, B. D. Rainford, T. J. Hicks and J. S. Kouvel, Phys. Rev. B 7, 218 (1973).

22. T. J. Hicks, B. Rainford, J. S. Kouvel, G. G. Low, and J. B. Comly, Phys. Rev. Lett. 22, 531 (1969).

23. H. A. Mook, Phys. Rev. 148, 495 (1966).

24. Y. Ito and J. Akimitsu, J. Phys. Soc. Japan 35, 1000 (1973).

25. J. W. Garland and A. Gonis, in Magnetism in Alloys, edited by P. A. Beck and J. T. Waber (TMS, AIME, New York, 1972), p. 79.

26. E. Balcar and W. Marshall, J. Phys. C 1, 966 (1968).

27. M. Hayase, M. Shiga and Y. Nakamura, J. Phys. Soc. Japan 34, 425 (1973).

28. B. N. Brockhouse, L. M. Corliss, and J. M. Hastings, Phys. Rev. 98, 1721 (1955).

29. J. Schelten and F. Hossfeld, J. Appl. Cryst. 4, 210 (1971).

30. B. Mozer, D. T. Keating and S. C. Moss, Phys. Rev. 175, 868 (1968).

31. G. P. Felcher, J. W. Garland, J. W. Cable and R. Medina, AIP Conf. Proc. 29, 331 (1976).

32. R. M. Moon, AIP Conf. Proc. 24, 925 (1975).

33. R. E. Watson, Phys. Rev. 119, 1934 (1960).

34. S. A. Ahern, M. J. C. Martin and W. A. Sucksmith, Proc. Roy. Soc. 248A, 145 (1958).

35. C. G. Robbins, H. Claus and P. A. Beck, J. Appl. Phys. 40, 2269 (1969).

36. J. P. Perrier, B. Tissier and R. Tournier, Phys. Rev. Lett. 24, 313 (1970).

37. S. Mishra, Int. J. Magn. 5, 363 (1974).

38. F. Acker and R. Huguenin, Phys. Lett. 38A, 343 (1972).

39. L. M. Roth, Phys. Rev. B 2, 740 (1970).

40. J. W. Garland, A. Gonis, J. S. Kouvel and A. T. Aldred, AIP Conf. Proc. 10, 1638 (1972).

41. H. Dvey-Aharon and M. Fibich, Phys. Rev. B 10, 287 (1974).

42. T. J. Hicks, Phys. Lett. 32A, 410 (1970).

43. S. W. Lovesey and W. Marshall, Proc. Phys. Soc. 89, 613 (1966).

44. G. S. Joyce, J. Phys. C: Solid St. Phys. 4, 153 (1971).

45. J. F. Cooke and H. L. Davis, AIP Conf. Proc. 10, 1218 (1973).

46. J. S. Kouvel and J. B. Comly, Phys. Rev. Lett. 24, 598 (1970).

47. J. W. Cable and R. A. Medina, Phys. Rev. B 13, 4868 (1976).

48. C. G. Robbins, H. Claus and P. A. Beck, Phys. Rev. Lett. 22, 1307 (1969).

49. P. C. Clapp and S. C. Moss, Phys. Rev. 142, 418 (1966).

VITA

Rodrigo Medina-Arocha was born in Caracas, Venezuela, on February 22, 1948. He attended elementary and high schools in Caracas graduating in 1965. He entered the Università degli Studi di Roma, Italy, and received the degree of Dottore in Fisica in 1970. From 1970 to 1972 he worked in the Departamento de Física of the Universidad Simón Bolívar of Caracas, first as a full time instructor and then part time after 1971 when he entered as a graduate student the Instituto Venezolano de Investigaciones Cientificas (IVIC). In 1972 he obtained from IVIC a scholarship to follow his graduate studies at the Georgia Institute of Technology. In 1974 he started his thesis research in the Oak Ridge National Laboratory.

In 1972 he married Paola Carpi, from Milan, Italy, and they now have a son, Humberto.